New Phytologist **Supporting Information**

Article title: Evolution of *L*-DOPA 4,5-dioxygenase activity allows for recurrent specialisation to betalain pigmentation in Caryophyllales

Authors: Hester Sheehan*, Tao Feng*, Nathanael Walker-Hale*, Samuel Lopez-Nieves, Boas Pucker, Rui Guo, Won C. Yim, Roshani Badgami, Alfonso Timoneda, Lijun Zhao, Helene Tiley, Dario Copetti, Michael J. Sanderson, John Cushman, Michael J. Moore, Stephen A. Smith, Samuel F. Brockington

Article acceptance date: 22 July 2019

The following Supporting Information is available for this article:

Figure S1 Taxon-labeled maximum likelihood *DODAα* gene tree with nucleotide branch lengths and support values. Sequences in a strongly supported *DODAα* clade from the full gene tree (Figs. **6**, **S6**) were extracted and a tree with support values was inferred with RAxML. Branch values are support from 200 rapid bootstrap replicates and the SH-aLRT, respectively (RBS/SH-aLRT). Branch lengths are expected substitutions per site (**pdf**).

Figure S2 Schematic of multi-gene binary vectors used in this study. *DODA* (pink text) was situated in second position and was the only element that varied between vectors. 35S, Cauliflower mosaic virus 35S promoter/terminator; act2, *Arabidopsis thaliana actin2* terminator; cDOPA-5GT, *Mirabilis jalapa cyclo-DOPA 5-O-glucosyltransferase*; CYP76AD1, *Beta vulgaris CYP76AD1*; DODA, *L*-DOPA 4,5-dioxygenase; Luciferase, *Photinus pyralis luciferase*; nos, *nopaline synthase* promoter/terminator; Ub10, *A. thaliana ubiquitin10* promoter.

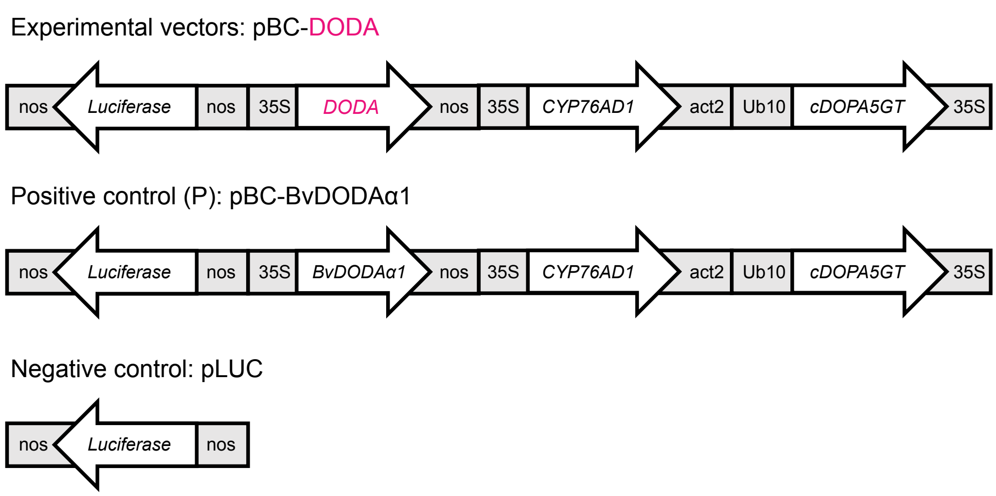

Figure S3 Maximum likelihood, time-calibrated genus-level phylogeny of Caryophyllales, inferred from seven nuclear and plastid markers. Sequences were collected using PyPHLAWD and a tree was inferred using RAxML. Branch lengths were scaled to time using treePL with fossil and secondary constraints. Branch labels give the rapid bootstrap support over 100 replicates, while node labels give the inferred node age in millions of years (**pdf**).

Figure S4 Ancestral state reconstruction of pigments by maximum likelihood and Bayesian inference via stochastic mapping. Tips are coloured according to pigmentation state: anthocyanin (blue), betalain (pink) and unknown (grey). Numbered arrows between states (A: anthocyanin, B: betalain) give the inferred rate of transition (myr-1) for maximum likelihood inference or the number of transitions between states on average across n = 1000 stochastic maps. Pie charts at nodes give the marginal scaled likelihood of each state for maximum likelihood inference or the posterior probability for Bayesian inference: **(a)** ancestral state reconstruction by Bayesian inference under the ER model; **(b)** ancestral state reconstruction by Bayesian inference under the ARD model; **(c)** ancestral state reconstruction by maximum likelihood under the (asymmetric) ER model; **(d)** ancestral state reconstruction by maximum likelihood under the (asymmetric) ARD model.

a)

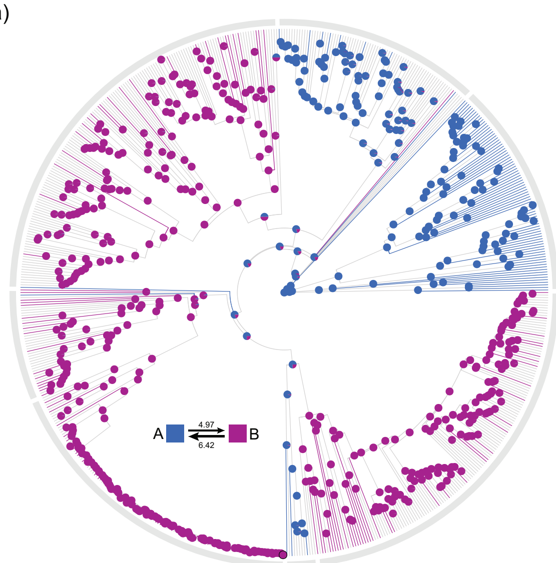

b)

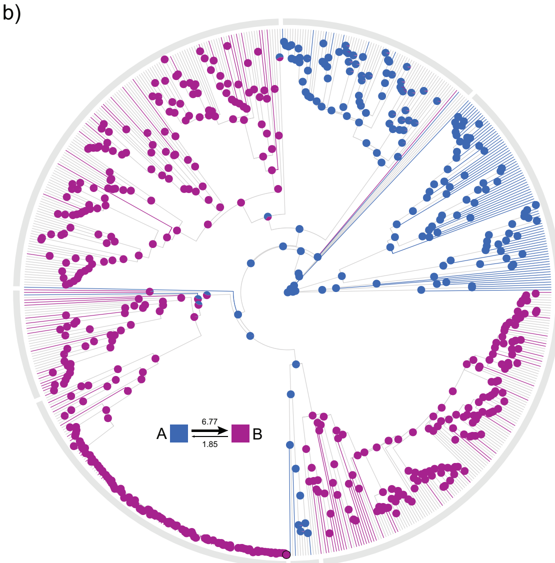

c)

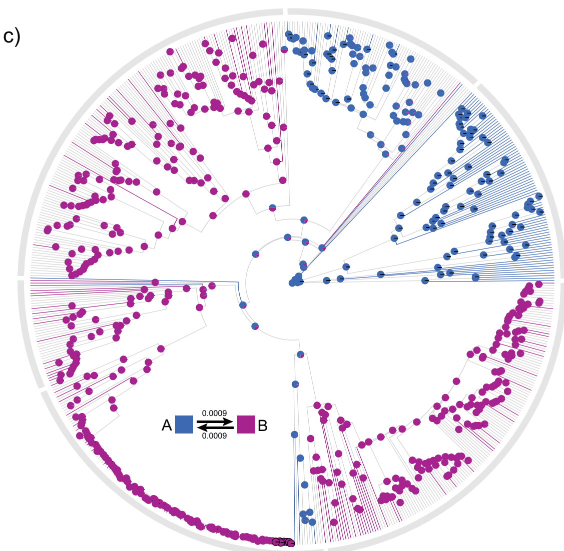

d)

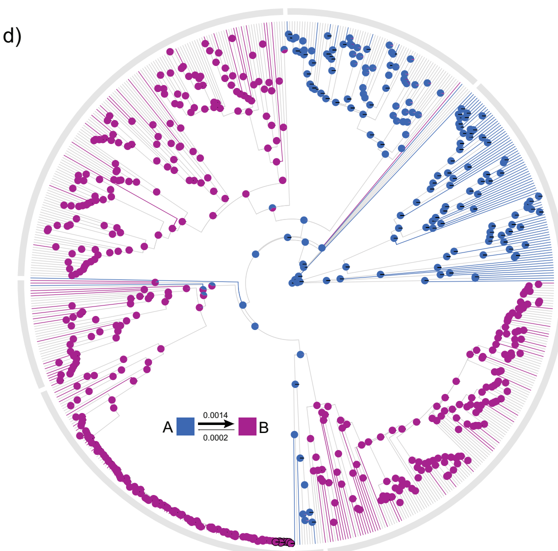

Figure S5 A simplified representation of the *DODA* gene tree. A maximum likelihood phylogeny of Caryophyllales *DODA* genes inferred from coding sequences derived from genome and transcriptome assemblies. Branch lengths are expected number of substitutions per site. Scale bar gives 0.2 expected substitutions per site. Branch labels are support values for major paralogous clades from rapid bootstrapping and the SH-like Approximate Likelihood Ratio Test, respectively, given as RBS/SH-aLRT. Putative major duplication nodes are highlighted with stars. Branches are coloured according to the putative pigmentation state of the taxa (blue = anthocyanin, pink = betalain).

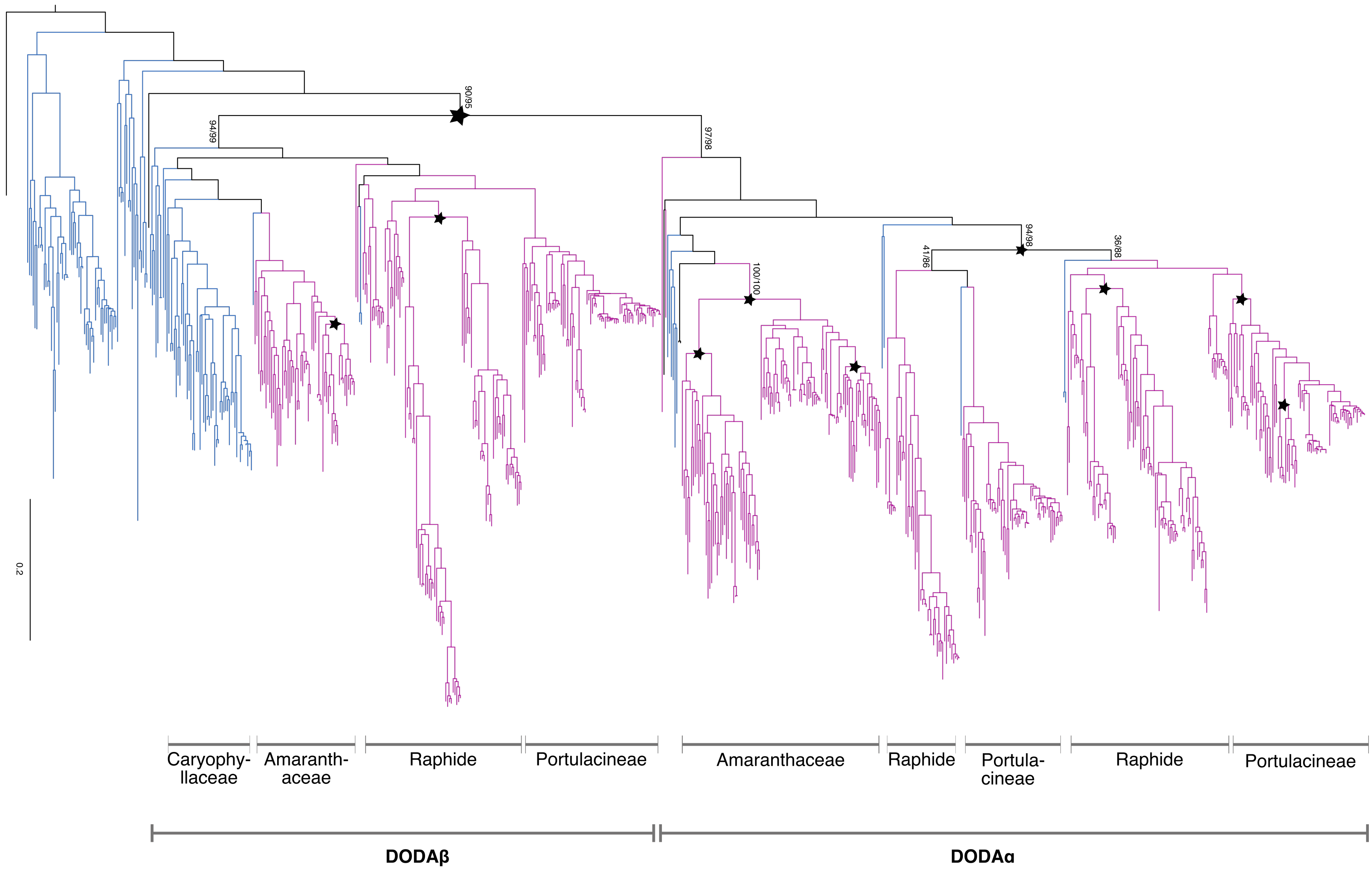

Caryophy-
llaceae
Amaranth-
aceae
Raphide
Portulacineae
Amaranthaceae
Raphide
Portula-
cineae
Raphide
Portulacineae
DODAβ
DODAα
90/95
94/99
97/98
100/100
41/86
94/98
36/88
0.2

Figure S6 Taxon-labeled maximum likelihood gene tree of *DODA* in Caryophyllales with support values. Sequences were collected from genome and transcriptome assemblies using a baited search approach and a tree with support values was inferred using RAxML. Branch labels are support from 200 rapid bootstrap replicates and SH-aLRT, respectively (RBS/SH-aLRT). Branch lengths are expected substitutions per site (**pdf**).

Figure S7 The *Corrigiola litoralis* and *Pollichia campestris DODAα* genes are putative pseudogenes. A schematic representation of the *DODAα* genes in *Corrigiola litoralis* and *Pollichia campestris* showing the mutations that affect their reading frame and introduce premature stop codons. *BvDODAα1* is included for comparison.

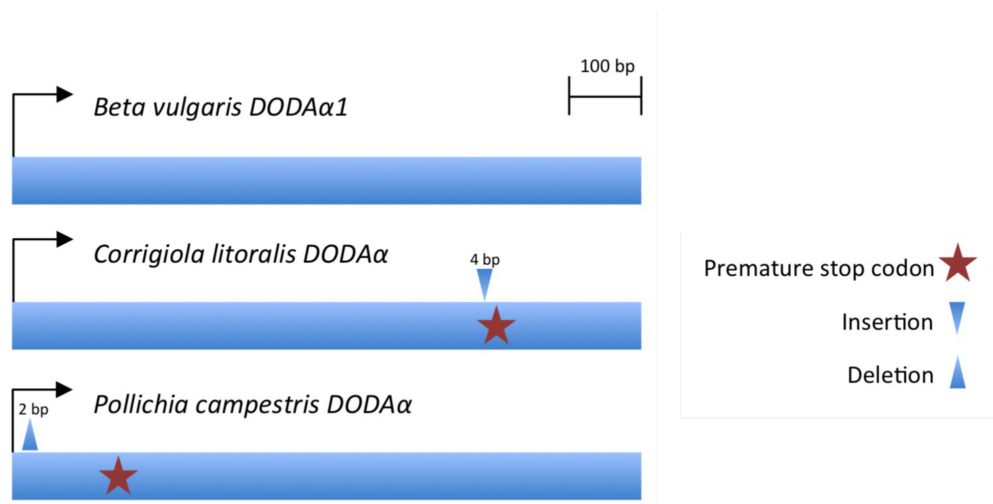

Figure S8 Functional characterisation of the full complement of *DODA* genes from *Stegnosperma halimifolium*. **(a)** Representative *Nicotiana bethamiana* leaves are shown from the agrobacterium infiltration of *DODA* genes from *S. halimifolium*. The *DODA* coding sequences were cloned into multi-gene constructs containing the other structural genes necessary for betacyanin production (*BvCYP76AD1*, *MjcDOPA-5GT*). The infiltration spots are labelled according to the DODA variant. The vector, pBC-BvDODAα1, was included as a positive control (P). pLUC was used as a negative control. **(b)** Betanin quantification in each of the leaves infiltrated with the *S. halimifolium DODA* genes and the pBC-BvDODAα1 positive control. "ShA3" corresponds to the leaf shown in **(a)**. **(c)** A representative HPLC trace is shown for each spot from the "ShA3" replicate. An external betanin standard (Betanin) was used to validate the retention time of betanin in these samples and calculate absolute amounts of betanin. The left peak is betanin and the right peak is its isomer, isobetanin.

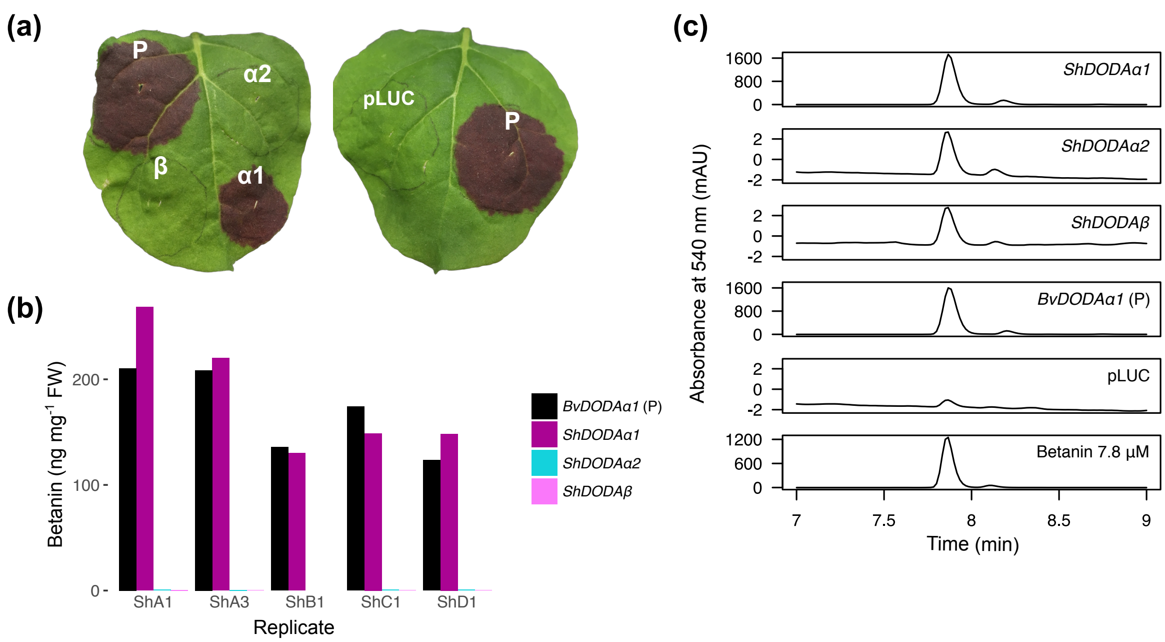

Figure S9 Functional characterisation of the full complement of *DODA* genes from *Beta vulgaris*.

(a) Representative *Nicotiana bethamiana* leaves are shown from the agrobacterium infiltration of *DODA* genes from *B. vulgaris*. The *DODA* coding sequences were cloned into multi-gene constructs containing the other structural genes necessary for betacyanin production (*BvCYP76AD1*, *MjcDOPA-5GT*). The infiltration spots are labelled according to the DODA variant. BvDODAα1 is represented by (P) for positive control which it served as throughout the study. pLUC was used as a negative control. nd, no data. **(b)** Betanin quantification in each of the leaves infiltrated with the *B. vulgaris DODA* genes. "25c2", "45c2" and "Bb1" correspond to the leaves shown in **(a)**. **(c)** A representative HPLC trace is shown for each spot of the samples shown in **(a)**. An external betanin standard (Betanin) was used to validate the retention time of betanin in these samples and calculate absolute amounts of betanin. The left peak is betanin and the right peak is its isomer, isobetanin.

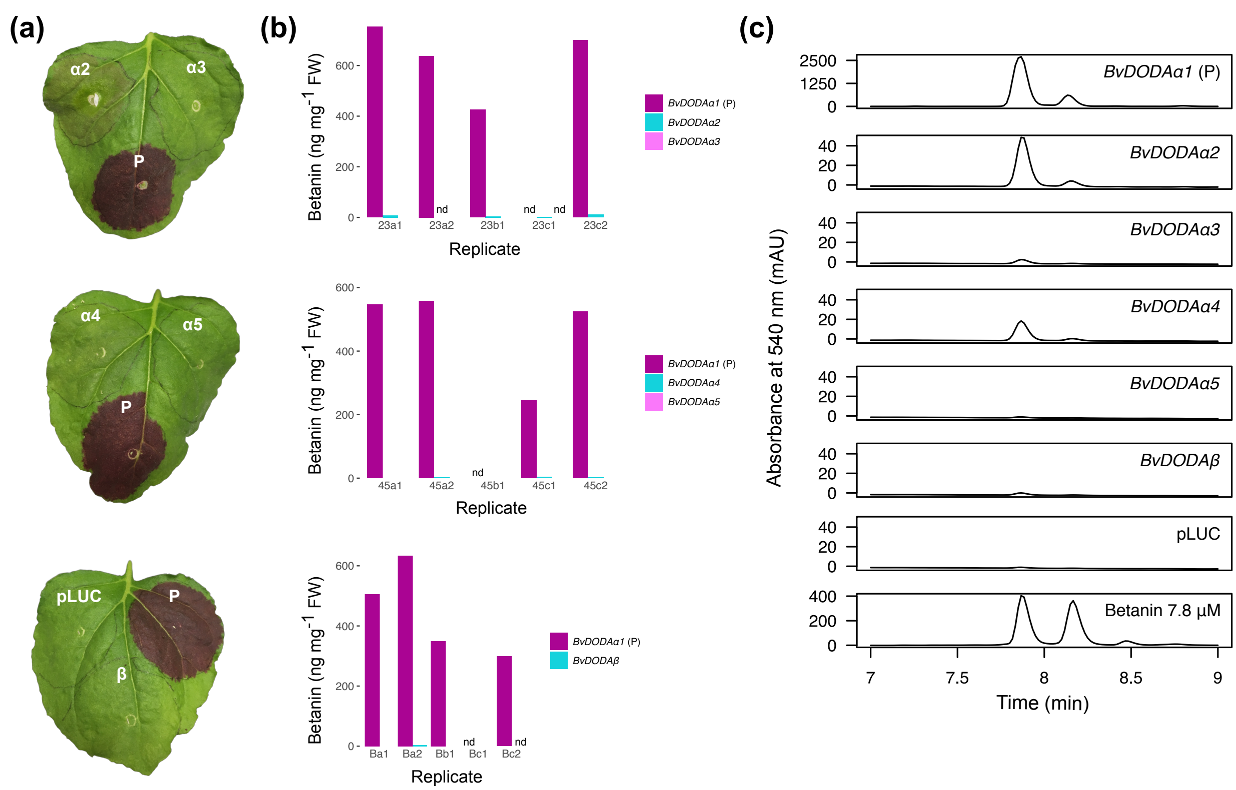

Figure S10 Functional characterisation of the full complement of *DODA* genes from *Mesembryanthemum crystallinum*. **(a)** Representative *Nicotiana bethamiana* leaves are shown from the agrobacterium infiltration of *DODA* genes from *M. crystallinum*. The *DODA* coding sequences were cloned into multi-gene constructs containing the other structural genes necessary for betacyanin production (*BvCYP76AD1*, *MjcDOPA-5GT*). The infiltration spots are labelled according to the DODA variant. The vector, pBC-BvDODAα1, was included as a positive control (P). pLUC was used as a negative control. **(b)** Betanin quantification in each of the leaves infiltrated with the *M. crystallinum DODA* genes and the pBC-BvDODAα1 positive control. "CB2" corresponds to the leaf shown in **(a)**. Unlike Figures S7, S8 and S10, for which the data were sampled at 4 days post-infiltration, these samples were taken at 5 days post-infiltration. **(c)** A representative HPLC trace is shown for each spot from the "CB2" replicate. An external betanin standard (Betanin) was used to validate the retention time of betanin in these samples and calculate absolute amounts of betanin. The left peak is betanin and the right peak is its isomer, isobetanin.

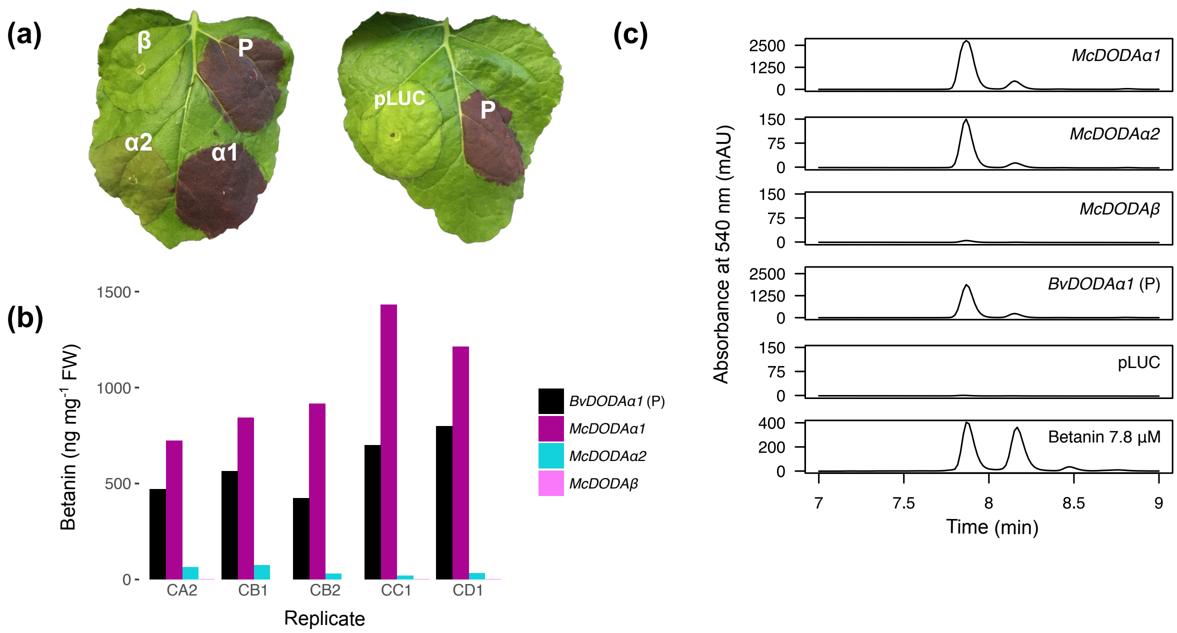

Figure S11 Functional characterisation of the full complement of *DODA* genes from *Carnegiea gigantea*. **(a)** Representative *Nicotiana bethamiana* leaves are shown from the agrobacterium infiltration of *DODA* genes from *C. gigantea*. The *DODA* coding sequences were cloned into multi-gene constructs containing the other structural genes necessary for betacyanin production (*BvCYP76AD1*, *MjcDOPA-5GT*). The infiltration spots are labelled according to the DODA variant. The vector, pBC-BvDODAα1, was included as a positive control (P). pLUC was used as a negative control. **(b)** Betanin quantification in each of the leaves infiltrated with the *C. gigantea DODA* genes and the pBC-BvDODAα1 positive control. "Cg2B1" corresponds to the leaf shown in **(a)**. **(c)** A representative HPLC trace is shown for each spot from the "Cg2B1" replicate. An external betanin standard (Betanin) was used to validate the retention time of betanin in these samples and calculate absolute amounts of betanin. The left peak is betanin and the right peak is its isomer, isobetanin.

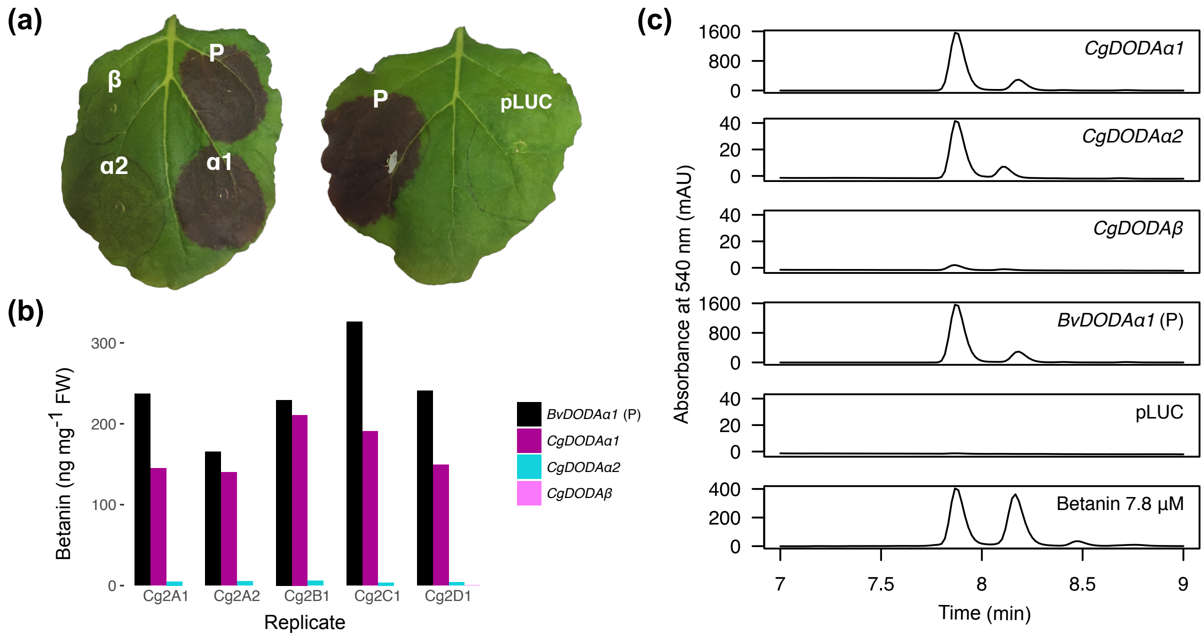

Figure S12 Functional characterisation of *DODAα* genes from anthocyanic Caryophyllales taxa. **(a)** *DODAα* genes from anthocyanic Caryophyllales taxa were cloned into multi-gene constructs containing the other structural genes necessary for betacyanin production (*BvCYP76AD1*, *MjcDOPA-5GT*) and agroinfiltrated into *Nicotiana benthamiana* leaves. Betanin quantification of agrobacterium-infiltrated *N. benthamiana* leaves was carried out using HPLC according to an external betanin standard. Each graph shows the quantification of betanin from each taxa's *DODAα* gene/s compared to the positive control, *BvDODAα1*. nd, no data. **(b)** A representative HPLC trace is shown for each infiltration spot. An external betanin standard (Betanin) was used to validate the retention time of betanin in these samples. The left peak is betanin and the right peak is its isomer, isobetanin.

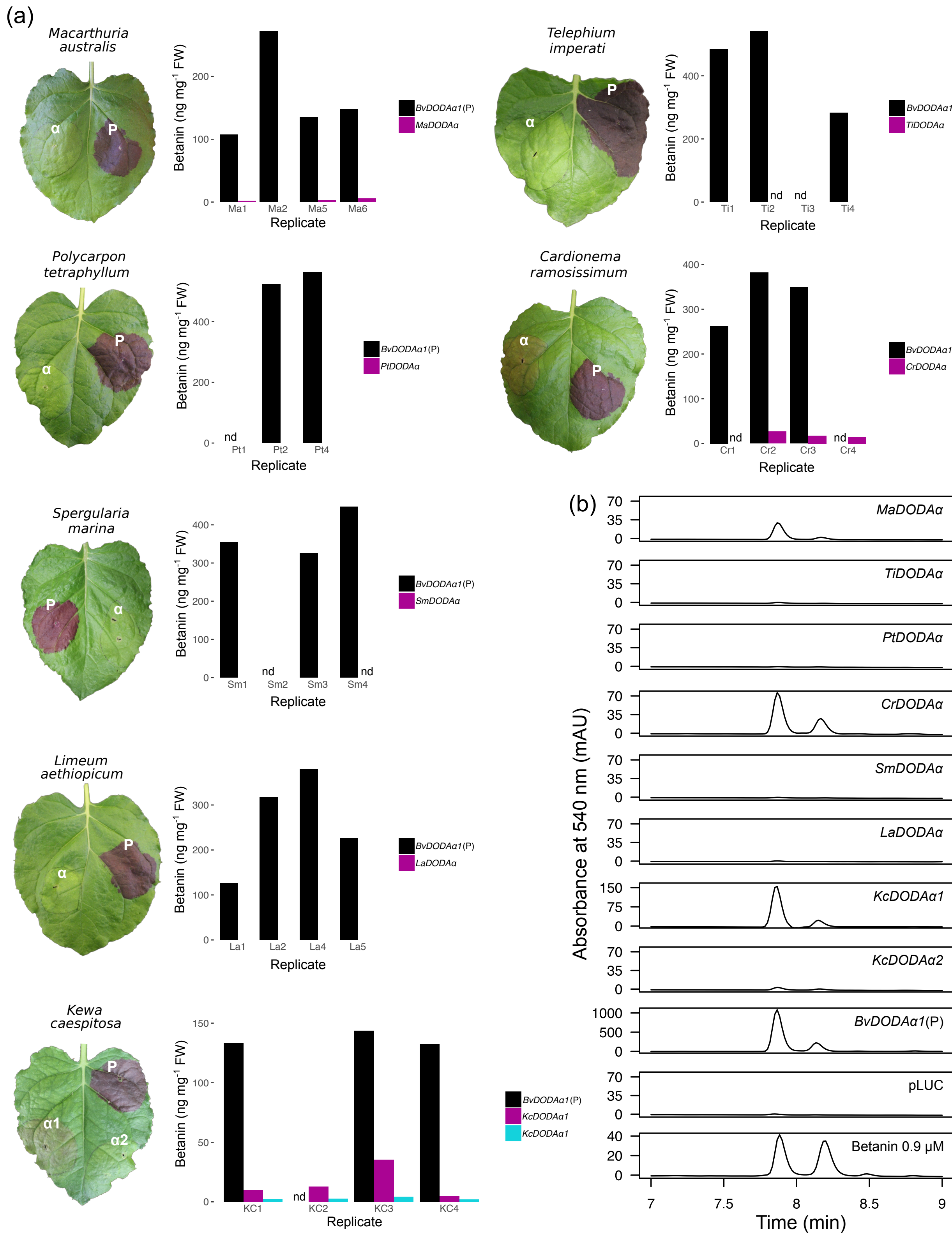

(a)
Macarthuria australis
α
P
Betanin (ng mg-1 FW)
Ma1 Ma2 Ma5 Ma6
Replicate
BvDODAα1(P)
MaDODAα
Telephium imperati
α
P
nd nd
Ti1 Ti2 Ti3 Ti4
TiDODAα
Polycarpon tetraphyllum
nd
Pt1 Pt2 Pt4
PtDODAα
Cardionema ramosissimum
Cr1 Cr2 Cr3 Cr4
CrDODAα
Spergularia marina
Sm1 Sm2 Sm3 Sm4
SmDODAα
Limeum aethiopicum
La1 La2 La4 La5
LaDODAα
Kewa caespitosa
α1
α2
KC1 KC2 KC3 KC4
KcDODAα1
KcDODAα1
(b)
MaDODAα
TiDODAα
PtDODAα
CrDODAα
SmDODAα
LaDODAα
KcDODAα1
KcDODAα2
BvDODAα1(P)
pLUC
Betanin 0.9 µM
Absorbance at 540 nm (mAU)
Time (min)
7 7.5 8 8.5 9

Figure S13 Taxon-labeled subsampled maximum likelihood *DODAα* gene tree with nucleotide branch lengths and support values. Sequences were subsampled from the *DODAα* gene tree using a custom script, and a tree with support values was inferred with RAxML. Branch labels are support from 200 rapid bootstrap replicates and the SH-aLRT, respectively (RBS/SH-aLRT). Branch lengths are expected substitutions per site (**pdf**).

Figure S14 Taxon-labeled subsampled maximum likelihood *DODAα* gene tree with codon branch lengths. The subsampled *DODAα* gene tree (Fig. **S13**) was used to optimize codon branch lengths under the best-fitting model of codon substitution (GY+F1X4+Γ(4)) and infer ancestral sequences using IQ-TREE. Branch lengths are expected substitutions per codon (**pdf**).

Figure S15 Taxon-labeled subsampled maximum likelihood *DODAα* gene tree with amino acid branch lengths**.** The subsampled *DODAα* gene tree (Fig. **S13**) was used to optimize amino acid branch lengths under the best-fitting model of amino acid substitution (JTT+Γ(4)) and infer ancestral sequences using IQ-TREE. Branch lengths are expected substitutions per site (**pdf**).

Figure S16 Ancestral amino acid sequence reconstruction for seven residues on subsampled *DODAα* gene tree. Ancestral sequences were inferred from the amino acid alignment of a subsample of *DODAα* sequences under the best-fitting model of amino acid substitution (JTT+Γ(4)) with IQ-TREE. Logo plots at nodes are the posterior probabilities of different states for the seven residues identified by Bean *et al.* (2018). Numbers mark the three putative origins of high levels of DODA activity.

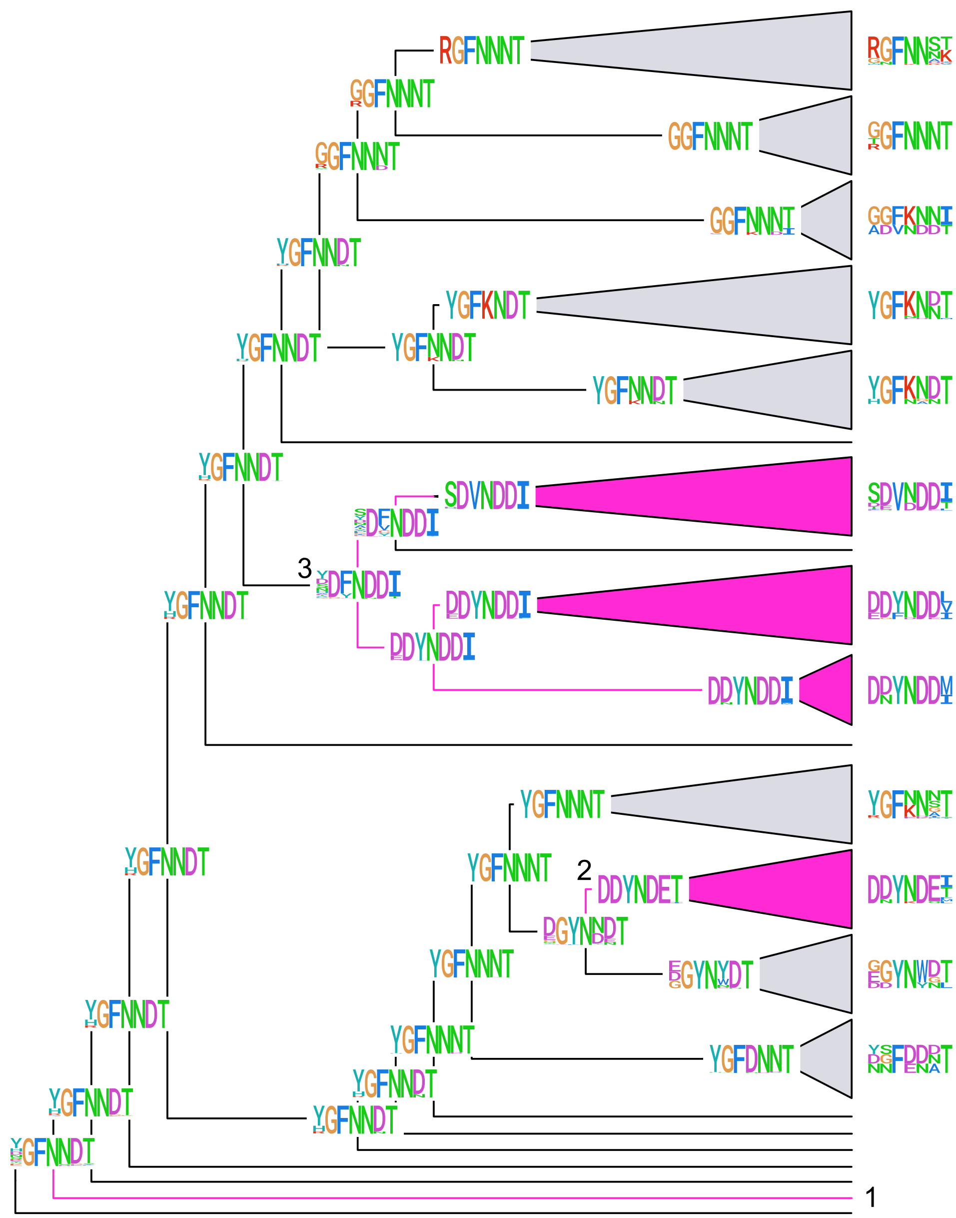

Table S1 Oligonucleotide primers used in this study

Name	Sequence (5' to 3')	Gene	Purpose
Bv_DODA_A_variant1F	ATGAAAATGATGAATGGAGAAG	*BvDODAα1*	Gene isolation
Bv_DODA_A_variant1R	CTAGGCTGAAGTGAACTTGTAG		
BvDODAα1_lvl0_F	TGAAGACATAATGAAAATGATGAATGGAGAAG		Goldengate cloning
BvDODAα1_lvl0_inR	TGAAGACATTGTATCTTCTACTGTTAATATTGG		
BvDODAα1_lvl0_inF	TGAAGACATTACACATCCATTAAGACCTTTC		
BvDODAα1_lvl0_R	TGAAGACATAAGCCTAGGCTGAAGTGAACTTGTAGGA		
Bv_DODA_A_variant2F	ATGGGTAGTGAAGATAACATCA	*BvDODAα2*	Gene isolation
Bv_DODA_A_variant2R	TTAGGTGGAAGTGAACTTGTAG		
BvDODAα2_lvl0_F	TTGAAGACATAATGGGTAGTGAAGATAACATC		Goldengate cloning
BvDODAα2_lvl0_R	TTGAAGACAAAAGCTTAGGTGGAAGTGAACTTGTAG		
Bv_DODA_A_variant3F	ATGGCACTTGATGATACAAAG	*BvDODAα3*	Gene isolation
Bv_DODA_A_variant3R	TTAGGTGGAAGTGAACTTATAGG		
BvDODAα3_lvl0_F	TTGAAGACATAATGGCACTTGATGATACAAAG		Goldengate cloning
BvDODAα3_lvl0_R	TTGAAGACAAAAGCTTAGGTGGAAGTGAACTTATAG		
Bv_DODA_B_variant2F	ATGGGTGGAGAGAAAATGAT	*BvDODAα4/ YTiBvDODAα4*	Gene isolation
Bv_DODA_B_variant2R	TCAGGTGGAAGTGAACTTGTA		
YTiBvDODAα4_lvl0_F	TTGAAGACATAATGGATGGAGAGAAAATGATC		Goldengate cloning
YTiBvDODAα4_lvl0_inR	TGAAGACATTGTGACCCAGGAGCCGGATAC		
YTiBvDODAα4_lvl0_inF	TGAAGACATTCACCAGAATTGGCAAAAAAG		
YTiBvDODAα4_lvl0_R	TTGAAGACAAAAGCTTAGGTGGAAGTGAACTTG		
HS3	TGGAACTCGTACTATGGCACT	*BvDODAα5*	Gene isolation
Bv_DODA_A_variant3R	TTAGGTGGAAGTGAACTTATAGG		
BvDODAα5_lvl0_F	TTGAAGACATAATGGCACTTGATGATTCAAAG		Goldengate cloning
BvDODAα5_lvl0_R	TTGAAGACAAAAGCTTAGGTGGAAGTGAACTTATAG		
Bv_DODA_B_variant1F	ATGAGTTATAATAGTGGTGCAAAAATTATG	*BvDODAβ*	Gene isolation
Bv_DODA_B_variant1R	TTAGTTCGGGGAGGTGAACT		
BvDODAβ_lvl0_F	TGAAGACATAATGAGTTATAATAGTGGTGCA		Goldengate cloning
BvDODAβ_lvl0_R	TGAAGACATAAGCTTAGTTCGGGGAGGTGAACTTGTAG		
MaDODAα_F1	ATGGATGGAACAGAGGAAAC	*MaDODAα*	Gene isolation
MaDODAα_R1	TCAAGTGGAAGTGAACTTGTAG		
MaDODAα_lvl0_F	TGAAGACATAATGGATGGAACAGAGGAAAC		Goldengate cloning
MaDODAα_lvl0_inF	TGAAGACATGGTTCTCACGATTTAGCGA		
MaDODAα_lvl0_inR	TGAAGACATAACCAGGTGCCGGATACT		
MaDODAα_lvl0_R	TGAAGACATAAGCTCAAGTGGAAGTGAACTTGT		
LaDODAα_F1	ATGACTAGCGAGACGTTCTAC	*LaDODAα*	Gene isolation
LaDODAα_R1	TCAGATGGAAGTGAACTTGTAG		
LaDODAα_lvl0_F	TGAAGACATAATGACTAGCGAGACGTTCTA		Goldengate cloning
LaDODAα_lvl0_inF	TGAAGACGAGGACGTTAATCATTACA		
LaDODAα_lvl0_inR	TGAAGACACGTCCTCATACCTTCCACTGA		
LaDODAα_lvl0_R	TGAAGACATAAGCTCAGATGGAAGTGAAC		
KcDODAα1_F1	GAAATCAAAAGGACACCGACA	*KcDODAα1*	Gene isolation
KcDODAα1_R1	CGCAGACAATAACAAAAAGTAACAC		
KcDODAα1_F2	GGACACCGACAGTCAGTAGCA		
KcDODAα1_R2	AACTAAACCACACGCAGACAA		
KcDODAα1_lvl0_F	TGAAGACATAATGGGTGCGGAGGACATGCT		Goldengate cloning
KcDODAα1_lvl0_inF1	TGAAGACATCCAGCTCAAGTATCCGGTTTCTGG		
KcDODAα1_lvl0_inF2	TGAAGACATGAAGGTATGAAGATGTGATTCATT		
KcDODAα1_lvl0_inR1	TGAAGACATCTGGTACATGGAAGCAGGGC		
KcDODAα1_lvl0_inR2	TGAAGACATCTTCCGCTGATCAGAGTTTC		
KcDODAα1_lvl0_R	TGAAGACATAAGCCTAGGTGGAGGTGAACTTAT		
KcDODAα2_F1	GCCAAACCCGTACCAAACCT	*KcDODAα2*	Gene isolation
KcDODAα2_R1	CCCCACTAAACAAGCAAAATG		
KcDODAα2_F2	ATGAATTGTGATTTGTGCCTTCCT		
KcDODAα2_R2	GCTTTAAGTGGAAGTGAACTTGTAGG		
KcDODAα2_lvl0_F	TGAAGACATAATGGGTGGTGGTGATGTGAT	*KcDODAα2*	Goldengate cloning
KcDODAα2_lvl0_inF1	TGAAGACATCCAGTTCAAGTACCCAGCTCCATG		
KcDODAα2_lvl0_inF2	TGAAGACATTCTTGACCACGCCTCATGGG		
KcDODAα2_lvl0_inF3	TGAAGACATGAAGGTATGAAGATGTGAACAATA		
KcDODAα2_lvl0_inR1	TGAAGACATCTGGTACATTTGAGCAGGGA		
KcDODAα2_lvl0_inR2	TGAAGACATAAGACCACGCTTCTTGTCTA		
KcDODAα2_lvl0_inR3	TGAAGACATCTTCCACTAGTTAGAGCTTC		
KcDODAα2_lvl0_R	TGAAGACATAAGCTTAAGTGGAAGTGAACTTGT		

Name	Sequence (5' to 3')	Gene	Purpose
CarDODAα F14	GAGACRTTCTTCATATCACAYGG	Caryophyllaceae *DODAα*	Gene isolation
CarDODAα R14	TCARCMGGAAGYGAACTTGTA		
CarDODAα F15	ATYCTYRTSRTCTCYGCTCA		
CarDODAα R15	TGYAAYGGRTAGAAGTGCTC		
CarDODAα_Fx	AWCAIYAGITISAAAATGGGC		
CarDODAα_F16	ATCCCKGTTTGTCAGCTCTCT		
CarDODAα_R16	AGAGAGCTGACAAACMGGGAT		
CarDODAα_F17	GAAGGTGTYCTCATMATYGGT		
CarDODAα_R17	ACCRATKATGAGRACACCTTC		
CarDODAα_R18	GAAGGGTGIGTGGYACTTCC		
CarDODAα_R19	CAKTSATCAAACTCIGCAGCCCA		
CarDODAα_R20	GTTTCCCARTGAGCRGAGA		
Cr3GPS1	AGGTGCAGGGTGAGGATGGTCGAGATG	*CrDODAα*	Gene isolation
Cr3GPS2	ACCCATATGTTGGGCCGTGTCCTTGA		
CrDODAα_F1	ATGACCTCTGAAGAAGCGAAAGAGATCA		
CrDODAα_R1	TCAGGTGGAAGTGAACTTATAGGAGCCA		
CrDODAα_lvl0_F	TGAAGACATAATGACCTCTGAAGAAGCGAA		Goldengate cloning
CrDODAα_lvl0_inF	TGAAGACATGATCTCCACAATTGGCAA		
CrDODAα_lvl0_inR	TGAAGACATGATCCAGGAGCTGGATACT		
CrDODAα_lvl0_R	TGAAGACATAAGCTCAGGTGGAAGTGAACTTAT		
PtDODAα_F1	ATGCATTGCTTAACTTTTCAACC	*PtDODAα*	Gene isolation
PtDODAα_F2	ATGATGAGAAGATGAACGAAAC		
PtDODAα_R1	TCAGGTGGAAGTGAATTTATAAG		
PtDODAα_F3	ATGATGATGCATTGCTTAACTTTTCAACC		
PtDODAα_R3	TCAGGTGGAAGTGAATTTATAAGAGCCA		
PtDODAα_lvl0_F	TGAAGACATAATGCATTGCTTAACTTTTCA		Goldengate cloning
PtDODAα_lvl0_R	TGAAGACATAAGCTCAGGTGGAAGTGAATT		
TiDODAα_F1	CCAACTACCAACATAAGCACT	*TiDODAα*	Gene isolation
TiDODAα_R1	TGGACAACAATGCAAAGGAG		
TiDODAα_F2	ACTGACTGTCTTGATCTGCCA		
TiDODAα_R2	TTGTTCTTGGCGATGTCAGTA		
TiDODAα_F3	CCACACTGGAAAAAGGCACAT		
TiDODAα_R3	GGAAAGCTGTCGAAATCGTAGA		
TiDODAα_R4	ATCAGTTTCCCAGTGAGC		
TiDODAα_F5	CACCAAAAACAGGTTTATCTAACG		
TiDODAα_R5	AAGAGGTCTAATTGCTCACGAC		
TiDODAα_F6	ATGAGTGACGAGCAAATGATC		
TiDODAα_R6	GCTGGAAGTGAATTTGTAGGAGG		
TiDODAα_lvl0_F	TGAAGACATAATGAGTGACGAGCAAATGAT		Goldengate cloning
TiDODAα_lvl0_inF1	TGAAGACATTCAGTTTAAGTACCCAGCTCCTGG		
TiDODAα_lvl0_inR1	TGAAGACATCTGATACATATAAGCAGGAA		
TiDODAα_lvl0_inF2	TGAAGACATGAAGGTATGAAGTAGTGAATAATTG		
TiDODAα_lvl0_inR2	TGAAGACATCTTCCTGTCGTCAGAGCTT		
TiDODAα_lvl0_inR	TGAAGACATAAGCTCAGCTGGAAGTGAATTTGT		
SmDODAα_F11	GCTACAAAATGGGCTGTCAAGAG	*SmDODAα*	Gene isolation
SmDODAα_F11'	ATGGGCTGTCAAGAGATGACT		
SmDODAα_R11	AGAGGTGGCATTGGAAGGGT		
SmDODAα_F12	TGGGCTGTCAAGAGATGACT		
SmDODAα_F12-2	ATGGGCTGTCAAGAGATGACT		
SmDODAα_R12	TCAACCGGAAGTGAACTTGT		
SmDODAα_lvl0_F	TGAAGACATAATGGGCTGTCAAGAGATGAC		Goldengate cloning
SmDODAα_lvl0_inF	TGAAGACGAGGACGTGAATAACTATG		
SmDODAα_lvl0_inR	TGAAGACACGTCCTCGTACCTTCCATTTG		
SmDODAα_lvl_R	TGAAGACATAAGCTCAACCGGAAGTGAACTTG		

Table S2 GenBank accession numbers for genes functionally characterised in this study

Species	***DODA* gene**	**Genbank ID**	**Alternative name**
Beta vulgaris	*BvDODAα1*	MN153194	BvDODA1 (Hatlestad *et al.*, 2012; HQ656027.1)
Beta vulgaris	*BvDODAα2*	MN153195	BvDODA2 (Hatlestad *et al.*, 2012; HQ656022.1); BvDODA (Christinet *et al.*, 2004; AJ583017)
Beta vulgaris	*BvDODAα3*	MN153196	*BvDODA2c (*Bean *et al., 2018)*
Beta vulgaris (YTiBv)	*BvDODAα4*	MN136228	BvDODA2b (Bean *et al.*, 2018)
Beta vulgaris	*BvDODAα5*	MN153197	BvDODA2d (Bean *et al.*, 2018)
Beta vulgaris	*BvDODAβ*	MN153198	-
Stegnosperma halimifolium	*ShDODAα1*	MN136219	-
Stegnosperma halimifolium	*ShDODAα2*	MN136220	-
Stegnosperma halimifolium	*ShDODAβ*	MN136221	-
Mesembryanthemum crystallinum	*McDODAα1*	MN136225	-
Mesembryanthemum crystallinum	*McDODAα2*	MN136226	-
Mesembryanthemum crystallinum	*McDODAβ*	MN136227	-
Carnegiea gigantea	*CgDODAα1*	MN136222	-
Carnegiea gigantea	*CgDODAα2*	MN136223	-
Carnegiea gigantea	*CgDODAβ*	MN136224	-
Spergularia marina	*SmDODAα*	MN153204	-
Cardionema ramosissimum	*CrDODAα*	MN153200	-
Telephium imperati	*TiDODAα*	MN153212	-
Polycarpon tetraphyllum	*PtDODAα*	MN153211	-
Macarthuria australis	*MaDODAα*	MN153205	-
Kewa caespitosa	*KcDODAα1*	MN153209	-
Kewa caespitosa	*KcDODAα2*	MN153210	-
Limeum aethiopicum	*LaDODAα*	MN153203	-
Pollichia campestris	*PcDODAα*	MN153206	-
Corrigiola litoralis	*ClDODAα*	MN153199	-

Table S3 Pigmentation status of 174 genera of Caryophyllales gathered from the literature. Pigments (anthocyanins: 0, betalains: 1) and literature reference (**xls**).

Table S4 Genome and transcriptome assemblies used in this study. Genome and transcriptome assemblies used both for individual *DODA* searches and automated baited homology searches. Species: family, genus and species, or genus and species for outgroup taxa; Code: the code used to identify this assembly in this study; Genome (transcriptome: 0, genome:1); Version: the assembly and/or annotation version; Source: the data depository or online database used to access the assembly; Reference: the literature reference for this assembly or underlying data; Notes: miscellaneous notes regarding this assembly; Reads accession: GenBank accession for raw reads; Assembly accession: accession number for GenBank-sourced assemblies; URL: a URL for quick access to assembly details (**xls**).

Table S5 *DODA* sequences used in *DODA* phylogeny. The *DODA* sequences included in the final gene tree are presented here (homologous sequence dataset, trimmed of sequences containing 50% or more gaps in the cleaned alignment). Taxon: the family, genus and species, or genus and species, of the taxa from which the sequence originated. Asterisks demarcate outgroup species; Sequence Identifier: the unique code used to identify this sequence in this study; Accession: accession for single sequences that are available on GenBank; Bait: was the sequence included in the initial bait set used to search genome and transcriptome assemblies (no: 0, yes: 1); in_ASR: was the sequence included in the subset of sequences used to infer ancestral *DODAα* sequences (no: 0, yes: 1) (**xls**).

Table S6 Details of *DODA* genes that have been functionally characterised from Caryophyllales species and mapped to the *DODA* gene tree

Species	Name	Accession	Publication	Method/Assay of functional characterisation	Corresponding phenotype
Stegnosperma halimifolium	*ShDODAα1*	MN136219	This study	Agroinfiltration in *Nicotiana benthamiana*	High levels of betanin
Stegnosperma halimifolium	*ShDODAα2*	MN136220	This study	Agroinfiltration in *N. benthamiana*	Marginal levels of betanin
Stegnosperma halimifolium	*ShDODAβ*	MN136221	This study	Agroinfiltration in *N. benthamiana*	Marginal levels of betanin
Beta vulgaris	*BvDODAα1*	MN153194	This study	Agroinfiltration in *N. benthamiana*	High levels of betanin
Beta vulgaris	*BvDODAα2*	MN153195	This study	Agroinfiltration in *N. benthamiana*	Weakly pigmented
Beta vulgaris	*BvDODAα3*	MN153196	This study	Agroinfiltration in *N. benthamiana*	No betanin present
Beta vulgaris	*BvDODAα4*	MN136228	This study	Agroinfiltration in *N. benthamiana*	Marginal levels of betanin
Beta vulgaris	*BvDODAα5*	MN153197	This study	Agroinfiltration in *N. benthamiana*	No betanin present
Beta vulgaris	*BvDODAβ*	MN153198	This study	Agroinfiltration in *N. benthamiana*	Marginal levels of betanin
Mesembryanthemum crystallinum	*McDODAα1*	MN136225	This study	Agroinfiltration in *N. benthamiana*	High levels of betanin
Mesembryanthemum crystallinum	*McDODAα2*	MN136226	This study	Agroinfiltration in *N. benthamiana*	Marginal levels of betanin
Mesembryanthemum crystallinum	*McDODAβ*	MN136227	This study	Agroinfiltration in *N. benthamiana*	Marginal levels of betanin
Carnegiea gigantea	*CgDODAα1*	MN136222	This study	Agroinfiltration in *N. benthamiana*	High levels of betanin
Carnegiea gigantea	*CgDODAα2*	MN136223	This study	Agroinfiltration in *N. benthamiana*	Marginal levels of betanin
Carnegiea gigantea	*CgDODAβ*	MN136224	This study	Agroinfiltration in *N. benthamiana*	Marginal levels of betanin
Macarthuria australis	*MaDODAα*	MN153205	This study	Agroinfiltration in *N. benthamiana*	Marginal levels of betanin
Limeum aethiopicum	*LaDODA*	MN153203	This study	Agroinfiltration in *N. benthamiana*	No betanin present
Kewa caespitosa	*KcDODAα1*	MN153209	This study	Agroinfiltration in *N. benthamiana*	Marginal levels of betanin
Kewa caespitosa	*KcDODAα2*	MN153210	This study	Agroinfiltration in *N. benthamiana*	Marginal levels of betanin
Polycarpon tetraphyllum	*PtDODA*	MN153211	This study	Agroinfiltration in *N. benthamiana*	No betanin present
Cardionema ramosissimum	*CrDODA*	MN153200	This study	Agroinfiltration in *N. benthamiana*	Marginal levels of betanin
Spergularia marina	*SmDODAα*	MN153204	This study	Agroinfiltration in *N. benthamiana*	No betanin present
Telephium imperati	*TiDODA*	MN153212	This study	Agroinfiltration in *N. benthamiana*	Marginal levels of betanin
Beta vulgaris	*BvDODAα1*	HQ656027.1	Bean *et al.*, 2018	Overexpression in acyanic *Beta vulgaris*	Yellow pigment
Beta vulgaris	*BvDODAα1*	HQ656027.1	Bean *et al.*, 2018	VIGS in *B. vulgaris*	Loss of pigmentation
Beta vulgaris	*BvDODAα1*	HQ656027.1	Bean *et al.*, 2018	Expression in *Saccharomyces cerevisiae*	DOPA-betaxanthin produced
Beta vulgaris	*BvDODAα2*	KM502868	Bean *et al.*, 2018	Overexpression in acyanic *B. vulgaris*	No yellow pigment
Beta vulgaris	*BvDODAα2*	KM502868	Bean *et al.*, 2018	VIGS in *B. vulgaris*	No loss of pigmentation
Beta vulgaris	*BvDODAα2*	KM502868	Bean *et al.*, 2018	Expression in *S. cerevisiae*	No DOPA-betaxanthin produced
Chenopodium quinoa	*CgDODA1*	XP_021769303	Imamura *et al.*, 2017	Agroinfiltration in *N. benthamiana*	High levels of betanin

Species	**Name**	**Accession**	**Publication**	**Method/Assay of functional characterisation**	**Corresponding phenotype**
Calandrinia mirabilis (Parakeelya mirabilis)	*PmDOD*	KF747352.1	Chung *et al.,* 2015	Biolistic transformation in *Antirrhinum majus* and *Allium cepa*	Strongly pigmented and autofluorescent
Calandrinia mirabilis (Parakeelya mirabilis)	*PmDOD-like*	KF747353.1	Chung *et al.,* 2015	Biolistic transformation in *A. majus* and *A. cepa*	Weakly pipgmented and autofluorescent
Ptilotus hybrid	*PhybDOD-like*	KF747354.1	Chung *et al.,* 2015	Biolistic transformation in *A. majus* and *A. cepa*	Weakly pipgmented and autofluorescent
Beta vulgaris	*BvDODAα1*	HQ656027.1	Chung *et al.,* 2015	Biolistic transformation in *A. majus*	Strongly pigmented and autofluorescent
Beta vulgaris	*BvDODA*	AJ583017	Chung *et al.,* 2015	Biolistic transformation in *A. majus*	Weakly pipgmented and autofluorescent
Dianthus superbus	*DsLigB*	JL390264	Chung *et al.,* 2015	Biolistic transformation in *A. majus*	No pigmentation
Beta vulgaris	*BvDODAα2*	AJ583017	Gandía-Herrero & García-Carmona, 2012	Recombinant expression in *Escherichia coli*	Forms betalamic acid from *L*-DOPA
Beta vulgaris	*BvDODAα1*	HQ656027.1	Hatlestad *et al.*, 2012	VIGS in *B. vulgaris*	Loss of pigmentation
Mirabilis jalapa	*MjDOD*	AB435372.1	Sasaki *et al.*, 2009	Recombinant expression in *E. coli*	Forms betalamic acid from *L*-DOPA
Portulaca grandiflora	*PgDODA*	AJ580598.1	Christinet *et al.*, 2004	Complementation of acyanic mutant	Restores pigmentation

Methods S1 Genome assembly

Sequencing of *Corrigiola litoralis*, *Limeum aethiopicum*, *Simmondsia chinensis* and *Spergula arvensis* was performed on a HiSeq X-Ten with one sample per lane. Processing of sequencing data, assembly via SOAPdenovo2 v2.04-r240 (Luo *et al.*, 2012), downstream processing, and gene prediction via AUGUSTUS v3.3 (Stanke *et al.*, 2008) was based on the previously described workflow (Pucker *et al.*, 2019). Assemblies of *C. litoralis* (ERS2294062), *L. aethiopicum* (ERZ869968), *S. chinensis* (ERZ497710), and *S. arvensis* (ERS2294061) are available at the EBI. AUGUSTUS v3.3 (Stanke *et al.*, 2008) was applied as previously described to predict protein-coding genes for these assemblies (Pucker *et al.*, 2019). Additionally, genome assemblies of *Lophocereus schottii* (GCA_002740545.1), *Pachycereus pringlei* (GCA_002740445.1), *Pereskia humboldtii* (GCA_002740485.1), *Stenocereus thurberi* (GCA_002740465.1), *Kewa caespitosa* (GCA_900322205), *Macarthuria australis* (GCA_900322265) and *Pharnaceum exiguum* (GCA_9003222385) were added to the downstream analysis.

Methods S2 Identification of full complements of *DODA* genes from betalain-pigmented species for functional analysis

Beta vulgaris

Using BLAST searches with the protein sequence of the previously characterized *BvDODAα1* (Hatlestad *et al.*, 2012), the *B. vulgaris* RefBeet (v1.2.2) genome contains six full-length and one partial annotated predicted genes that have homology to *DODA* (Brockington *et al.*, 2015; Table **S2**). For this publication, the full-length *DODA* genes were isolated from *B. vulgaris* 'Bolivar' with one exception. *BvDODAα4* was amplified from cDNA from leaf tissue of *B. vulgaris* sugarbeet 'YTiBv' using the YTiBv-1.0 genome assembly (scaffold13748: 34334..33958, 34808..34555, 32278..32057; Table **S4**).

The partial *DODA* sequence (XM_010676273.2) was also investigated. The first exon of *BvDODAα6* has no protein homology to other *DODAs* and the second exon is half the expected size. BLAST searches were carried out upstream of the annotated regions, up to the next annotated gene, in order to search for regions of homology to *DODA* sequences. Some extra sequences were found but they were either very short, or in a different reading frame. Because this transcript does not encode a full-length DODA protein, they likely represent incomplete tandem duplications or pseudogenisations and thus were not investigated further for DODA-specific function.

Carnegiea gigantea

Four *DODA* genes were identified by performing a BLAST search using representative *DODA* genes from *B. vulgaris* in the *C. gigantea* genome assembly SGPv1.3 and its corresponding predicted genes (Table **S4**; PRJNA318822; Copetti *et al.*, 2017). The predicted transcript, Cgig1_02616, was found to be composed of coding sequences corresponding to two *DODA* genes, referred to as *CgDODAα2* and *CgDODAβ*. These were manually annotated by comparison with other *DODA* genes, and by comparison with RNAseq datasets (Copetti *et al.*, 2017). Cgig1_02617 is directly upstream from the Cgig1_02616 annotation. The predicted exons only have partial homology, and contain in-frame stop codons. By BLASTing the sequence between this transcript and Cgig1_02616, an extra region with homology to exon 3 of the *DODA* genes could be found, but this region contains two stop codons and a frame-shift. There is also no RNAseq evidence for this gene, altogether indicating that this is likely a pseudogenisation arising after tandem duplication of *CgDODAα2*, and thus this gene was not investigated further.

Mesembryanthemum crystallinum

Amino acid sequences of the *B. vulgaris DODAs* were retrieved from the RefBeet v1.2 genome database (Dohm *et al.*, 2014). The amino acid sequences were mapped against the *M. crystallinum* genome annotation (W. C. Yim, unpublished) using TBLASTN from BLAST (Camacho *et al.*, 2009). The identified CDS sequences were manually curated and confirmed by RNAseq reads support.

Methods S3 Phylogeny of Caryophyllales

To enable trait reconstruction across the order, we generated a comprehensive genus-level species tree for Caryophyllales using publicly-available sequence data compiled by PyPHLAWD (Smith & Walker, 2019). Briefly, we ran PyPHLAWD with default configurations for the whole of Caryophyllales on the GenBank 'pln' division (downloaded 26/11/2018), used find_good_clusters.py to select the most well-sampled markers, and sampled a single species per genus with the greatest sequence-wise coverage across these markers, ensuring that no infraspecific taxa were selected. Then we reran PyPHLAWD on the same database, restricting the list of retrieved sequences to the selected taxa. We carried forward the seven most well-sampled markers for phylogenetic reconstruction. These were the nucleotide marker ITS and the plastid markers *rbcL*, *matK*, *rps16*, *trnL*-*trnF*, *rpl16* and *atpB*-*rbcL*. Alignments were concatenated into a supermatrix and a maximum likelihood phylogeny was inferred using RAxML v8.2.12 (Stamatakis, 2014). We partitioned the alignment by gene and used the overall algorithm to conduct 100 Rapid Bootstrap replicates and thereafter a thorough maximum likelihood tree search from 10 bootstrap starting trees under the GTR+Γ model of sequence evolution. In order to reflect current understanding of the Caryophyllales phylogeny, we incorporated a relatively strong constraint following the MQSST topology inferred from phylogenomic data by Walker *et al.* (2018) and a placement of *Lophiocarpus* and *Corbichonia* following Thulin *et al.* (2016, 2018). However, we did not enforce the non-monophyly of the non-core recovered in the former as it was weakly supported. We rooted the phylogeny with the clade of non-core Caryophyllales. To scale the branches of our species tree to time, we used treePL (Smith & O'Meara, 2012), which uses a penalized likelihood framework (Sanderson, 2002) and is capable of handling large trees. To constrain our inference, we used the same fossil and secondary constraints as Smith *et al.* (2018), and sources therein, except that the root age was that from the UCLN clock analysis of Magallón *et al.* (2015; max 107.13 mya, min 102.5 mya). We conducted a priming analysis to determine the best starting values and used cross-validation to determine the optimal smoothing parameter.

Methods S4 Pigment reconstruction

Pigment data at genus level resolution was used to reconstruct the evolution of betalain pigmentation on the time-calibrated genus-level phylogeny of Caryophyllales. We surveyed the literature for pigment data and determined the pigmentation status of 174 genera, classifying them as anthocyanin-pigmented, betalain-pigmented, or unknown (Table **S3**). We further assumed that all non-core Caryophyllales are anthocyanin pigmented. Where only one species in a genus was tested, we assumed that its pigmentation status was generalizable. We reconstructed pigmentation as a binary trait using maximum likelihood (Pagel, 1994, 1999) and stochastic mapping (Nielsen, 2002; Huelsenbeck *et al.*, 2003) with the ape and phytools R packages, respectively (Revell, 2012; R Core Team, 2019; Paradis & Schliep, 2019). For both methods, we implemented two different forms of the Mk model (Pagel, 1994; Lewis, 2001): i) Symmetric, allowing equal rates (ER) of evolution from anthocyanin to betalain and *vice versa* and ii) Asymmetric (or All Rates Different; ARD), allowing a different rate of evolution from anthocyanin to betalain than from betalain to anthocyanin. Unknown taxa were given an equal likelihood of being in either state. In the maximum likelihood case, we compared model performance with AIC scores (Burnham & Anderson, 2002). For stochastic mapping, we enforced a strong prior that the root of the tree was anthocyanin-pigmented, although prior sensitivity analyses indicated that this was not the cause of our results.

Methods S5 Gene tree of Caryophyllales *DODA* genes

We compiled a dataset of publicly available and early release genome and transcriptome assemblies. We collected 39 ingroup and outgroup genomes from public repositories and added the full complement of 297 ingroup transcriptomes from Walker *et al.* (2018). We supplemented these with 9 genomes newly assembled or reannotated for this study and 11 Aizoaceae transcriptomes from L. Zhao (unpublished). Full dataset details can be found in Table **S4**. To infer the gene tree of DODA in Caryophyllales, we employed the baited homologue approach following Lopez-Nieves *et al.* (2018). Scripts for this analysis were downloaded from https://bitbucket.org/yangya/adh_2016 and received minor modifications; all scripts can be found at https://github.com/NatJWalker-Hale/DODA. We used a bait set of previously analyzed *DODA* genes from the literature (Table **S5**). In order to include baits from Caryophyllaceae that were putative pseudogenes, we aligned the baits with MACSE v2.03 (Ranwez *et al.*, 2018) with defaults and replaced any codons containing inferred deletions with ambiguities (-), such that the inframe proteins had ambiguities at this site. First, we clustered similar amino acid sequences in transcriptomes using CD-HIT v4.7 (-n 5 -c 0.995) (Fu *et al.*, 2012). We conducted similarity searches using SWIPE v2.1.0 (Rognes, 2011), retaining the top 10 candidates. We then conducted three rounds of automated iterative alignment inference and tree inference with MAFFT v7.409 (Katoh & Standley, 2013) and FastTree v2.1.10 (Price *et al.*, 2010), monophyletic masking and trimming, before a round of manual curation to produce the homologue set. Manual curation involved adding three baits which were inferred on long branches and erroneously removed during the pipeline, removing redundant sequences where another sequence from the same loci was longer, masking monophyletic transcriptome sequences to remove isoforms, removing sequences on long branches and removing sequences that had radically divergent phylogenetic placement indicative of error. Amino acid sequences of the final homologue set were aligned with MAFFT v7.409 (Katoh & Standley, 2013) (--genafpair --maxiterate 1000), and coding sequences were aligned to the amino acids with the function pxaa2cdn from the phyx package (Brown *et al.*, 2017). The dataset was cleaned of columns with 90% or more missing data using pxclsq from phyx (-p 0.1). Sequences containing over 50% gaps in the cleaned alignment were removed. The resulting dataset was realigned, coding sequences were realigned and cleaned (pxclsq -p 0.1), and RAxML v8.2.12 was used to conduct 200 Rapid Bootstrap replicates and thereafter a thorough maximum likelihood tree search from 10 different bootstrap starting trees, under the GTR+Γ(4) model of sequence evolution. We also used RAxML to NNI-optimize the tree and generate support values from the SH-like Approximate Likelihood Ratio Test (SH-aLRT) (Guindon *et al.*, 2010). If a better tree was found during NNI optimization, we carried this tree forward and remapped bootstrap replicates to this topology. Finally, we extracted a strongly-supported clade of *DODAα* genes following Brockington *et al.* (2015), and realigned, re-inferred a maximum likelihood tree and generated support using the same approach as previously (Fig. **S1**).

Methods S6 Ancestral Sequence Reconstruction

To create a sequence dataset computationally and numerically tractable for ancestral sequence reconstruction, we used custom python scripts (subsample_by_paralog.py; https://github.com/NatJWalker-Hale/DODA) to subsample the *DODAα* gene tree (Fig. **S1**), using a strategy designed to maintain within-paralogue diversity. To do this, we used the species overlap algorithm implemented in ete3 (Huerta-Cepas *et al.*, 2016) to break the tree into paralogues, before sampling within each paralogue such that every family had at least its longest sequence in the cleaned alignment or longest sequences proportional to its representation in that paralogue within the original dataset. We created a final dataset of 198 sequences, ensuring that a representative of all functionally characterized *DODAα* loci was included. We aligned and inferred an ML tree for this dataset using the same approach as above (Fig**. S13**). Marginal ancestral sequence reconstructions were conducted on this tree for codons and amino acids in IQ-TREE v1.6.10 (Nguyen *et al.*, 2015; Kalyaanamoorthy *et al.*, 2017) under the best-fitting substitution model (-m MFP -msub nuclear -mrate E,G,R -asr). We tested both the cleaned (pxclsq -p 0.1) and uncleaned alignment. However, because IQ-TREE does not conduct ancestral inference of gaps, we carried forward results from the cleaned alignment. Probabilities of ancestral states at each node for the sites identified by Bean *et al.* (2018) were summarised using logo plots created with the R package ggseqlogo (Wagih, 2017; R Core Team, 2019). Codon reconstructions were visualised as their translated amino acids by summing over the probabilities of redundant codons.

References

Bean A, Sunnadeniya R, Akhavan N, Campbell A, Brown M, Lloyd A, Lloyd A. **2018**. Gain-of-function mutations in beet DODA2 identify key residues for betalain pigment evolution. *New Phytologist* **219**: 287–296.

Brockington SF, Yang Y, Gandía-Herrero F, Covshoff S, Hibberd JM, Sage RF, Wong GKS, Moore MJ, Smith SA. **2015**. Lineage-specific gene radiations underlie the evolution of novel betalain pigmentation in Caryophyllales. *New Phytologist* **207**: 1170–1180.

Brown JW, Walker JF, Smith SA. **2017**. Phyx: phylogenetic tools for unix. *Bioinformatics* **33**: 1886–1888.

Burnham KP, Anderson D. **2002**. *Model Selection and Multimodel Inference: A Practical Information-Theoretic Approach*. New York: Springer-Verlag.

Camacho C, Coulouris G, Avagyan V, Ma N, Papadopoulos J, Bealer K, Madden TL. **2009**. BLAST+: architecture and applications. *BMC Bioinformatics* **10**: 421.

Christinet L, Burdet FX, Zaiko M, Hinz U, Zrÿd J-P. **2004**. Characterization and functional identification of a novel plant 4,5-extradiol dioxygenase involved in betalain pigment biosynthesis in *Portulaca grandiflora*. *Plant Physiology* **134**: 265–274.

Chung H-H, Schwinn KE, Ngo HM, Lewis DH, Massey B, Calcott KE, Crowhurst R, Joyce DC, Gould KS, Davies KM, *et al.* 2015. Characterisation of betalain biosynthesis in *Parakeelya* flowers identifies the key biosynthetic gene DOD as belonging to an expanded LigB gene family that is conserved in betalain-producing species. *Frontiers in Plant Science* **6**: 1–16.

Copetti D, Búrquez A, Bustamante E, Charboneau JLM, Childs KL, Eguiarte LE, Lee S, Liu TL, McMahon MM, Whiteman NK, *et al.* 2017. Extensive gene tree discordance and hemiplasy shaped the genomes of North American columnar cacti. *Proceedings of the National Academy of Sciences* **114**: 12003–12008.

Cuénoud P, Savolainen V, Chatrou LW, Powell M, Grayer RJ, Chase MW. 2002. Molecular phylogenetics of Caryophyllales based on nuclear 18S rDNA and plastid rbcL, atpB, and matK DNA sequences. *American Journal of Botany* **89**: 132–144.

Clement JS, Mabry TJ, Wyler H, Dreiding AS. 1994. Chemical Review and Evolutionary Significance of the Betalains. In: Behnke H-D, Mabry TJ, eds. Caryophyllales: Evolution and Systematics. Berlin, Heidelberg: Springer Berlin Heidelberg, 247–261.

Dohm JC, Minoche AE, Holtgräwe D, Capella-Gutiérrez S, Zakrzewski F, Tafer H, Rupp O, Sörensen TR, Stracke R, Reinhardt R, *et al.* 2014. The genome of the recently domesticated crop plant sugar beet (*Beta vulgaris*). *Nature* **505**: 546–9.

Fu L, Niu B, Zhu Z, Wu S, Li W. **2012**. CD-HIT: accelerated for clustering the next-generation sequencing data. *Bioinformatics* **28**: 3150–3152.

Gandía-Herrero F, García-Carmona F. **2012**. Characterization of recombinant *Beta vulgaris* 4,5-DOPA-extradiol-dioxygenase active in the biosynthesis of betalains. *Planta* **236**: 91–100.

Guindon S, Dufayard JF, Lefort V, Anisimova M, Hordijk W, Gascuel O. **2010**. New algorithms and methods to estimate maximum-likelihood phylogenies: assessing the performance of PhyML 3.0. *Systematic Biology* **59**: 307–321.

Hatlestad GJ, Sunnadeniya RM, Akhavan NA, Gonzalez A, Goldman IL, McGrath JM, Lloyd AM. **2012**. The beet R locus encodes a new cytochrome P450 required for red betalain production. *Nature Genetics* **44**: 816–820.

Huelsenbeck JP, Nielsen R, Bollback JP. **2003**. Stochastic mapping of morphological characters. *Systematic Biology* **52**: 131–158.

Huerta-Cepas J, Serra F, Bork P. **2016**. ETE 3: reconstruction, analysis, and visualization of phylogenomic data. *Molecular Biology and Evolution* **33**: 1635–1638.

Imamura T, Takagi H, Miyazato A, Ohki S, Mizukoshi H, Mori M. **2018**. Isolation and characterization of the betalain biosynthesis gene involved in hypocotyl pigmentation of the allotetraploid *Chenopodium quinoa*. *Biochemical and Biophysical Research Communications* **496**: 280–286.

Kalyaanamoorthy S, Minh BQ, Wong TKF, Von Haeseler A, Jermiin LS. **2017**. ModelFinder: fast model selection for accurate phylogenetic estimates. *Nature Methods* **14**: 587–589.

Katoh K, Standley DM. **2013**. MAFFT multiple sequence alignment software version 7: improvements in performance and usability. *Molecular Biology and Evolution* **30**: 772–80.

Lewis PO. **2001**. A likelihood approach to estimating phylogeny from discrete morphological character data. *Systematic Biology* **50**: 913-925.

Lopez-Nieves S, Yang Y, Timoneda A, Wang M, Feng T, Smith SA, Brockington SF, Maeda HA. **2018**. Relaxation of tyrosine pathway regulation underlies the evolution of betalain pigmentation in Caryophyllales. *New Phytologist* **217**: 896–908.

Luo R, Liu B, Xie Y, Li Z, Huang W, Yuan J, He G, Chen Y, Pan Q, Liu Y, *et al.* **2012**. SOAPdenovo2: an empirically improved memory-efficient short-read de novo assembler. *GigaScience* **1**: 18.

Magallón S, Gómez-Acevedo S, Sánchez-Reyes LL, Hernández-Hernández T. **2015**. A metacalibrated time-tree documents the early rise of flowering plant phylogenetic diversity. *New Phytologist* **207**: 437–453.

Nguyen LT, Schmidt HA, Von Haeseler A, Minh BQ. **2015**. IQ-TREE: a fast and effective stochastic algorithm for estimating maximum-likelihood phylogenies. *Molecular Biology and Evolution* **32**: 268–274.

Nielsen R. **2002**. Mapping mutations on phylogenies. *Systematic Biology* **51**: 729–739.

Pagel M. **1994**. Detecting correlated evolution on phylogenies: a general method for the comparative analysis of discrete characters. *Proceedings of the Royal Society B* **255**: 37–45.

Pagel M. **1999**. The maximum likelihood approach to reconstructing ancestral character states of discrete characters on phylogenies. *Systematic Biology* **48**: 612–622.

Paradis E, Schliep K. **2019**. Ape 5.0: an environment for modern phylogenetics and evolutionary analyses in R. *Bioinformatics* **35**: 526–528.

Price MN, Dehal PS, Arkin AP. **2010**. FastTree 2 - approximately maximum-likelihood trees for large alignments. *PLoS ONE* **5**: e9490.

Pucker B, Feng T, Brockington SF. **2019**. Next generation sequencing to investigate genomic diversity in

Caryophyllales. *bioRxiv*. doi: https://doi.org/10.1101/646133

R Core Team. **2019**. R: a language and environment for statistical computing. Version 3.6.1. R Foundation for Statistical Computing, Vienna, Austria. URL http://www.R-project.org/

Ranwez V, Douzery EJP, Cambon C, Chantret N, Delsuc F. **2018**. MACSE v2: toolkit for the alignment of coding sequences accounting for frameshifts and stop codons. *Molecular Biology and Evolution* **35**: 2582–2584.

Revell LJ. **2012**. phytools: an R package for phylogenetic comparative biology (and other things). *Methods in Ecology and Evolution* **3**: 217–223.

Rognes T. **2011**. Faster Smith-Waterman database searches with inter-sequence SIMD parallelisation. *BMC Bioinformatics* **12**: 221.

Sanderson MJ. 2002. Estimating absolute rates of molecular evolution and divergence times: a penalized likelihood approach. *Molecular Biology and Evolution* **19**: 101–109.

Sasaki N, Abe Y, Goda Y, Adachi T, Kasahara K, Ozeki Y. **2009**. Detection of DOPA 4,5-dioxygenase (DOD) activity using recombinant protein prepared from *Escherichia coli* cells harboring cDNA encoding DOD from *Mirabilis jalapa*. *Plant and Cell Physiology* **50**: 1012–1016.

Smith SA, Brown JW, Yang Y, Bruenn R, Drummond CP, Brockington SF, Walker JF, Last N, Douglas NA, Moore MJ. **2018**. Disparity, diversity, and duplications in the Caryophyllales. *New Phytologist* **217**: 836–854.

Smith SA, O'Meara BC. **2012**. TreePL: divergence time estimation using penalized likelihood for large phylogenies. *Bioinformatics* **28**: 2689–2690.

Smith SA, Walker JF. **2019**. PyPHLAWD: a python tool for phylogenetic dataset construction. *Methods in Ecology and Evolution* **10**: 104–108.

Stamatakis A. **2014**. RAxML version 8: a tool for phylogenetic analysis and post-analysis of large phylogenies. *Bioinformatics* **30**: 1312–1313.

Stanke M, Diekhans M, Baertsch R, Haussler D. **2008**. Using native and syntenically mapped cDNA alignments to improve *de novo* gene finding. *Bioinformatics* **24**: 637–644.

Thulin M, Larsson A, Edwards EJ, Moore AJ. **2018**. Phylogeny and systematics of *Kewa* (Kewaceae) . *Systematic Botany* **43**: 689–700.

Thulin M, Moore AJ, El-Seedi H, Larsson A, Christin PA, Edwards EJ. **2016**. Phylogeny and generic delimitation in Molluginaceae, new pigment data in Caryophyllales, and the new family Corbichoniaceae. *Taxon* **65**: 775–793.

Wagih O. **2017**. Ggseqlogo: a versatile R package for drawing sequence logos. *Bioinformatics* **33**: 3645–3647.

Walker JF, Yang Y, Feng T, Timoneda A, Mikenas J, Hutchinson V, Edwards C, Wang N, Ahluwalia S, Olivieri J, *et al.* 2018. From cacti to carnivores: improved phylotranscriptomic sampling and hierarchical homology inference provides further insight to the evolution of Caryophyllales. *American Journal of Botany* **105**: 446–462.

New Phytologist Supporting Information Figs S1, S3, S6 & S13–S15

Article title: Evolution of L-DOPA 4,5-dioxygenase activity allows for recurrent specialisation to betalain pigmentation in Caryophyllales

Authors: Hester Sheehan*,Tao Feng*, Nathanael Walker-Hale*, Samuel Lopez-Nieves, Boas Pucker, Rui Guo, Won C. Yim, Roshani Badgami, Alfonso Timoneda, Lijun Zhao, Helene Tiley, Dario Copetti, Michael J. Sanderson, John C. Cushman, Michael J. Moore, Stephen A. Smith and Samuel F. Brockington

Article acceptance date: 22 July 2019

Figure S1

Figure S3

Figure S6

Figure S13

Figure S14

Cactaceae_Ariocarpus_retusus_79378
Cactaceae_Ferocactus_latispinus_93070
Cactaceae_Astrophytum_myriostigma_61758
Cactaceae_Coryphantha_maiztablensis_14139
Cactaceae_Lophocereus_schottii_01053643.1_g24146.t1
Cactaceae_Pachycereus_gatesii_47798
Cactaceae_Carnegia_gigantea_Cgig1_02616_CgDODAa
Cactaceae_Hylocereus_lemairei_polyrhizus_15461
Cactaceae_Echinopsis_aurea_71662
Cactaceae_Stetsonia_coryne_29106
Cactaceae_Gymnocalycium_mihanovichii_4025
Cactaceae_Eriosyce_wageneckii_45808
Cactaceae_Rhipsalis_baccifera_subsp_baccifera_39769
Cactaceae_Leuenbergeria_bleo_24123
Cactaceae_Leuenbergeria_lychnidiflora_27067
Cactaceae_Puna_bonnieae_78434
Cactaceae_Pereskia_grandifolia_19396
Portulacaceae_Portulaca_pilosa_4065
Portulacaceae_Portulaca_suffruticosa_3459
Portulacaceae_Portulaca_oleracea_SRA_58254
Portulacaceae_Portulaca_umbraticola_867
Portulacaceae_Portulaca_oleracea_SRA_58253
Portulacaceae_Portulaca_pilosa_4066
Montiaceae_Claytonia_virginica_13434
Montiaceae_Montia_chamissoi_34252
Montiaceae_Parakeelya_mirabilis_KF747353.1_cds_AIS23504.1_1
Montiaceae_Cistanthe_grandiflora_35834
Montiaceae_Phemeranthus_parviflorus_44522
Anacampserotaceae_Grahamia_kurtzii_63330
Didiereaceae_Portulacaria_afra_26390
Talinaceae_Talinum_paniculatum_6206
Didiereaceae_Alluaudia_dumosa_54606
Didiereaceae_Alluaudia_procera_61471
Basellaceae_Anredera_cordifolia_54197
Basellaceae_Anredera_cordifolia_7613
Didiereaceae_Alluaudia_dumosa_88966
Anacampserotaceae_Talinopsis_frutescens_62
Portulacaceae_Portulaca_cryptopetala_21090
Aizoaceae_Conophytum_uviforme_DN8524_c0_g2_i2
Aizoaceae_Fenestraria_aurantiaca_DN5550_c0_g1_i2
Aizoaceae_Juttandinteria_kovismontana_DN23254_c0_g1_i1
Aizoaceae_Glotyphyllum_uncatum_DN16698_c0_g1_i1
Aizoaceae_Mesembryanthemum_crystallinum_Mecry_081870_CDS_-_McDODAa2
Aizoaceae_Sesuvium_portulacastrum_24229
Aizoaceae_Sesuvium_verrucosum_71221
Aizoaceae_Trianthema_portulacastrum_SRA_26095
Nyctaginaceae_Abronia_bigelovii_58480
Nyctaginaceae_Abronia_glabrifolia_94439
Nyctaginaceae_Abronia_latifolia_31660
Nyctaginaceae_Abronia_carletonii_43101
Nyctaginaceae_Abronia_fragrans_77996
Nyctaginaceae_Abronia_umbellata_2819
Nyctaginaceae_Tripterocalyx_carneus_27782
Nyctaginaceae_Tripterocalyx_crux_maltae_21128
Nyctaginaceae_Acleisanthes_lanceolata_35964
Nyctaginaceae_Acleisanthes_purpusiana_47741
Nyctaginaceae_Acleisanthes_obtusa_36152
Nyctaginaceae_Nyctaginia_capitata_64734
Nyctaginaceae_Mirabilis_jalapa_KM502866.1_cds_AJD87535.1_1
Nyctaginaceae_Mirabilis_pringlei_58425
Nyctaginaceae_Mirabilis_multiflora_39438
Nyctaginaceae_Commicarpus_scandens_67003
Nyctaginaceae_Guapira_obtusata_56229
Nyctaginaceae_Pisonia_umbellifera_16244
Petiveriaceae_Monococcus_echinophorus_38989
Phytolaccaceae_Anisomeria_littoralis_3120
Phytolaccaceae_Phytolacca_dioica_31478
Phytolacaceae_Phytolacca_americana_AB451869.1_cds_BAH66635.1_1
Agdestidaceae_Agdestis_clematidea_2489
Sarcobataceae_Sarcobatus_vermiculatus_MJM_70860
Petiveriaceae_Seguieria_aculeata_59340
Nyctaginaceae_Boerhavia_purpurascens_5655
Nyctaginaceae_Boerhavia_torreyana_11639
Nyctaginaceae_Okenia_hypogea_74016
Nyctaginaceae_Anulocaulis_annulatus_4970
Nyctaginaceae_Tripterocalyx_crux_maltae_689
Nyctaginaceae_Acleisanthes_chenopodioides_14610
Nyctaginaceae_Acleisanthes_lanceolata_30806
Nyctaginaceae_Acleisanthes_purpusiana_48633
Nyctaginaceae_Mirabilis_jalapa_c44693_g1_i1_97_870_minus
Phytolacaceae_Phytolacca_americana_AB451870.1_cds_BAH66636.1_1
Phytolaccaceae_Anisomeria_littoralis_32336
Kewaceae_Kewa_caespitosa_DODAa2
Cactaceae_Maihueniopsis_conoidea_9246
Cactaceae_Pterocactus_tuberosus_67194
Cactaceae_Puna_bonnieae_41816
Cactaceae_Tephrocactus_articulatus_83622
Cactaceae_Salmiopuntia_salmiana_54166
Cactaceae_Tacinga_lilae_22876
Cactaceae_Opuntia_arenaria_90271
Cactaceae_Grusonia_bradtiana_43949
Cactaceae_Echinopsis_aurea_86484
Cactaceae_Matucana_aurantiaca_46823
Cactaceae_Stetsonia_coryne_38827
Cactaceae_Ariocarpus_retusus_1063
Cactaceae_Astrophytum_asterias_10417
Cactaceae_Carnegia_gigantea_Cgig1_18485_CgDODAa1
Cactaceae_Rhipsalis_baccifera_subsp_baccifera_64009
Anacampserotaceae_Talinopsis_frutescens_1849
Portulacaceae_Portulaca_grandiflora_AJ580598.1_cds_CAE45178.1_1
Portulacaceae_Portulaca_oleracea_SRA_9226
Talinaceae_Talinum_fruticosum_30303
Didiereaceae_Didierea_madagascariensis_62799
Didiereaceae_Didierea_trollii_34754
Didiereaceae_Alluaudia_dumosa_74255
Montiaceae_Claytonia_nevadensis_33794
Montiaceae_Lewisia_nevadensis_75879
Montiaceae_Parakeelya_mirabilis_KF747352.1_cds_AIS23503.1_1
Montiaceae_Calandrinia_grandiflora_or_procumbens_20222
Montiaceae_Calyptridium_pygmaeum_73640
Montiaceae_Phemeranthus_parviflorus_44523
Basellaceae_Basella_alba_24974
Kewaceae_Kewa_caespitosa_DODAa1
Nyctaginaceae_Acleisanthes_lanceolata_32010
Nyctaginaceae_Acleisanthes_purpusiana_35413
Nyctaginaceae_Acleisanthes_obtusa_33521
Nyctaginaceae_Abronia_umbellata_59901
Nyctaginaceae_Commicarpus_scandens_9477
Nyctaginaceae_Cyphomeris_gypsophiloides_16268
Nyctaginaceae_Mirabilis_jalapa_AB435372.1_cds_BAG80686.1_1
Nyctaginaceae_Mirabilis_pringlei_33165
Nyctaginaceae_Mirabilis_multiflora_44341
Nyctaginaceae_Colignonia_ovalifolia_2171
Nyctaginaceae_Salpianthus_purpurascens_91019
Petiveriaceae_Monococcus_echinophorus_54274
Petiveriaceae_Rivina_humilis_15447
Phytolaccaceae_Anisomeria_littoralis_57030
Phytolaccaceae_Phytolacca_americana_24205
Agdestidaceae_Agdestis_clematidea_15017
Gisekiaceae_Gisekia_pharnaceoides_439
Aizoaceae_Conophytum_uviforme_DN6421_c0_g3_i2
Aizoaceae_Fenestraria_aurantiaca_DN19219_c0_g2_i2
Aizoaceae_Mesembryanthemum_crystallinum_Mecry_173920_CDS_-_McDODAa1
Limeaceae_Limeum_aethiopicum_DODAa
Chenopodiaceae_Anabasis_articulata_53850
Chenopodiaceae_Haloxylon_ammodendron_38175
Chenopodiaceae_Kali_collina_24381
Chenopodiaceae_Caroxylon_vermiculatum_87166
Chenopodiaceae_Eokochia_saxicola_53502
Chenopodiaceae_Suaeda_fruticosa_9702
Chenopodiaceae_Suaeda_linearis_1939
Chenopodiaceae_Kalidium_cuspidatum_23308
Amaranthaceae_Polycnemum_majus_4766
Chenopodiaceae_Spinacia_oleracea_Spo27232
Chenopodiaceae_Atriplex_hortensis_62354
Chenopodiaceae_Atriplex_sp_21625
Chenopodiaceae_Extriplex_californica_28742
Chenopodiaceae_Proatriplex_pleiantha_11096
Chenopodiaceae_Chenopodiastrum_murale_51976
Chenopodiaceae_Chenopodium_giganteum_Chenopodium_amaranticolor_14731
Chenopodiaceae_Oxybasis_rubra_6048
Chenopodiaceae_Krascheninnikovia_lanata_42646
Chenopodiaceae_Agriophyllum_squarrosum_33278
Amaranthaceae_Alternanthera_philoxeroides_86014
Amaranthaceae_Tidestromia_lanuginosa_35934
Amaranthaceae_Iresine_arbuscula_42789
Amaranthaceae_Iresine_rhizomatosa_38768
Amaranthaceae_Gossypianthus_lanuginosus_16893
Amaranthaceae_Guilleminea_densa_var_aggregata_15913
Amaranthaceae_Ptilotus_exaltatus_hyb_KF747354.1_cds_AIS23505.1_1
Amaranthaceae_Froelichia_latifolia_25043
Amaranthaceae_Tidestromia_lanuginosa_35931
Amaranthaceae_Alternanthera_philoxeroides_86019
Amaranthaceae_Nelsia_quadrangula_44223
Chenopodiaceae_Beta_vulgaris_XM_010675993.2_cds_XP_010674295.1_1
Chenopodiaceae_Beta_vulgaris_XM_010675996.2_cds_XP_010674298.1_1
Chenopodiaceae_Beta_vulgaris_HQ656022.1_cds_AET43288.1_1
Amaranthaceae_Amaranthus_hypochondriacus_HQ889614.1_cds_ADZ48644.1_1
Amaranthaceae_Amaranthus_tricolor_KP165399.1_cds_AJW81119.1_1
Amaranthaceae_Gossypianthus_lanuginosus_40105
Amaranthaceae_Tidestromia_lanuginosa_37237
Amaranthaceae_Nelsia_quadrangula_55789
Amaranthaceae_Amaranthus_cruentus_KM592963.1_cds_AJD87538.1_1
Amaranthaceae_Amaranthus_tricolor_18737
Chenopodiaceae_Caroxylon_vermiculatum_73089
Chenopodiaceae_Eokochia_saxicola_70762
Chenopodiaceae_Arthrocnemum_macrostachyum_57682
Chenopodiaceae_Beta_vulgaris_HQ656027.1_cds_AET43293.1_1
Chenopodiaceae_Chenopodium_quinoa_AUR62022991-RA
Chenopodiaceae_Spinacia_oleracea_XM_021991322.1_cds_XP_021847014.1_1
Chenopodiaceae_Chenopodium_quinoa_XM_021876909.1_cds_XP_021732601.1_1
Chenopodiaceae_Extriplex_californica_9479
Chenopodiaceae_Krascheninnikovia_lanata_31913
Amaranthaceae_Froelichia_latifolia_26247
Amaranthaceae_Tidestromia_lanuginosa_4485
Chenopodiaceae_Beta_vulgaris_XM_010676009.2_cds_XP_010674311.1_1
Chenopodiaceae_Oxybasis_rubra_10367
Chenopodiaceae_Oxybasis_rubra_36364
Caryophyllaceae_Cardionema_ramosissimum_DODAa
Caryophyllaceae_Polycarpon_tetraphyllum_DODAa
Caryophyllaceae_Spergularia_marina_DODAa
Achatocarpaceae_Achatocarpus_gracilis_8287
Caryophyllaceae_Telephium_imperatii_DODAa
Macarthuriaceae_Macarthuria_australis_DODAa
Stegnospermataceae_Stegnosperma_halimifolium_1183
Microteaceae_Microtea_debilis_174616
Stegnospermataceae_Stegnosperma_halimifolium_50374
Chenopodiaceae_Chenopodium_quinoa_AUR62006956-RA
0.4

Figure S15

Cactaceae_Ariocarpus_retusus_79378
Cactaceae_Ferocactus_latispinus_93070
Cactaceae_Astrophytum_myriostigma_61758
Cactaceae_Coryphantha_maiztablensis_14139
Cactaceae_Lophocereus_schottii_01053643.1.g24146.t1
Cactaceae_Pachycereus_gatesii_47798
Cactaceae_Carnegia_gigantea_Cgig1_02616_CgDODAa
Cactaceae_Hylocereus_lemairei_polyrhizus_15461
Cactaceae_Echinopsis_aurea_71662
Cactaceae_Stetsonia_coryne_29106
Cactaceae_Gymnocalycium_mihanovichii_4025
Cactaceae_Eriosyce_wageneckii_45808
Cactaceae_Rhipsalis_baccifera_subsp_baccifera_39769
Cactaceae_Leuenbergeria_bleo_24123
Cactaceae_Leuenbergeria_lychnidiflora_27067
Cactaceae_Puna_bonnieae_78434
Cactaceae_Pereskia_grandifolia_19396
Portulacaceae_Portulaca_pilosa_4065
Portulacaceae_Portulaca_suffruticosa_3459
Portulacaceae_Portulaca_oleracea_SRA_58254
Portulacaceae_Portulaca_umbraticola_867
Portulacaceae_Portulaca_oleracea_SRA_58253
Portulacaceae_Portulaca_pilosa_4066
Montiaceae_Claytonia_virginica_13434
Montiaceae_Montia_chamissoi_34252
Montiaceae_Parakeelya_mirabilis_KF747353.1_cds_AIS23504.1_1
Montiaceae_Cistanthe_grandiflora_35834
Montiaceae_Phemeranthus_parviflorus_44522
Anacampserotaceae_Grahamia_kurtzii_63330
Didiereaceae_Portulacaria_afra_26390
Talinaceae_Talinum_paniculatum_6206
Didiereaceae_Alluaudia_dumosa_54606
Didiereaceae_Alluaudia_procera_61471
Basellaceae_Anredera_cordifolia_54197
Basellaceae_Anredera_cordifolia_7613
Didiereaceae_Alluaudia_dumosa_88966
Anacampserotaceae_Talinopsis_frutescens_62
Portulacaceae_Portulaca_cryptopetala_21090
Aizoaceae_Conophytum_uviforme_DN8524_c0_g2_i2
Aizoaceae_Fenestrania_aurantiaca_DN5550_c0_g1_i2
Aizoaceae_Juttadinteria_kovismontana_DN23254_c0_g1_i1
Aizoaceae_Glotyphylum_uncatum_DN16698_c0_g1_i1
Aizoaceae_Mesembryanthemum_crystallinum_Mecry_081870_CDS_-_McDODAa2
Aizoaceae_Sesuvium_portulacastrum_24229
Aizoaceae_Sesuvium_verrucosum_71221
Aizoaceae_Trianthema_portulacastrum_SRA_26095
Nyctaginaceae_Abronia_bigelovii_58480
Nyctaginaceae_Abronia_glabrifolia_94439
Nyctaginaceae_Abronia_latifolia_31660
Nyctaginaceae_Abronia_carletonii_43101
Nyctaginaceae_Abronia_fragrans_77996
Nyctaginaceae_Abronia_umbellata_2819
Nyctaginaceae_Tripterocalyx_carneus_27782
Nyctaginaceae_Tripterocalyx_crux_maltae_21128
Nyctaginaceae_Acleisanthes_lanceolata_35964
Nyctaginaceae_Acleisanthes_purpusiana_47741
Nyctaginaceae_Acleisanthes_obtusa_36152
Nyctaginaceae_Nyctaginia_capitata_64734
Nyctaginaceae_Mirabilis_jalapa_KM502866.1_cds_AJD87535.1_1
Nyctaginaceae_Mirabilis_pringlei_58425
Nyctaginaceae_Mirabilis_multiflora_39438
Nyctaginaceae_Commicarpus_scandens_67003
Nyctaginaceae_Guapira_obtusata_56229
Nyctaginaceae_Pisonia_umbellifera_16244
Petiveriaceae_Monococcus_echinophorus_38989
Phytolaccaceae_Anisomeria_littoralis_3120
Phytolaccaceae_Phytolacca_dioica_31478
Phytolaccaceae_Phytolacca_americana_AB451869.1_cds_BAH66635.1_1
Agdestidaceae_Agdestis_clematidea_2489
Sarcobataceae_Sarcobatus_vermiculatus_MJM_70860
Petiveriaceae_Seguieria_aculeata_59340
Nyctaginaceae_Boerhavia_purpurascens_5655
Nyctaginaceae_Boerhavia_torreyana_11639
Nyctaginaceae_Okenia_hypogea_74016
Nyctaginaceae_Anulocaulis_annulatus_4970
Nyctaginaceae_Tripterocalyx_crux_maltae_689
Nyctaginaceae_Acleisanthes_chenopodioides_14610
Nyctaginaceae_Acleisanthes_lanceolata_30806
Nyctaginaceae_Acleisanthes_purpusiana_48633
Nyctaginaceae_Mirabilis_jalapa_c44693_g1_i1_97_870_minus
Phytolaccaceae_Phytolacca_americana_AB451870.1_cds_BAH66636.1_1
Phytolaccaceae_Anisomeria_littoralis_32336
Kewaceae_Kewa_caespitosa_DODAa2
Cactaceae_Maihueniopsis_conoidea_9246
Cactaceae_Pterocactus_tuberosus_67194
Cactaceae_Puna_bonnieae_41816
Cactaceae_Tephrocactus_articulatus_83622
Cactaceae_Salmiopuntia_salmiana_54166
Cactaceae_Tacinga_lilae_22876
Cactaceae_Opuntia_arenaria_90271
Cactaceae_Grusonia_bradtiana_43949
Cactaceae_Echinopsis_aurea_86484
Cactaceae_Matucana_aurantiaca_46823
Cactaceae_Stetsonia_coryne_38827
Cactaceae_Ariocarpus_retusus_1063
Cactaceae_Astrophytum_asterias_10417
Cactaceae_Carnegia_gigantea_Cgig1_18485_CgDODAa1
Cactaceae_Rhipsalis_baccifera_subsp_baccifera_64009
Anacampserotaceae_Talinopsis_frutescens_1849
Portulacaceae_Portulaca_grandiflora_AJ580598.1_cds_CAE45178.1_1
Portulacaceae_Portulaca_oleracea_SRA_9226
Talinaceae_Talinum_fruticosum_30303
Didiereaceae_Didierea_madagascariensis_62799
Didiereaceae_Didierea_trollii_34754
Didiereaceae_Alluaudia_dumosa_74255
Montiaceae_Claytonia_nevadensis_33794
Montiaceae_Lewisia_nevadensis_75879
Montiaceae_Parakeelya_mirabilis_KF747352.1_cds_AIS23503.1_1
Montiaceae_Calandrinia_grandiflora_or_procumbens_20222
Montiaceae_Calyptridium_pygmaeum_73640
Montiaceae_Phemeranthus_parviflorus_44523
Basellaceae_Basella_alba_24974
Kewaceae_Kewa_caespitosa_DODAa1
Nyctaginaceae_Acleisanthes_lanceolata_32010
Nyctaginaceae_Acleisanthes_purpusiana_35413
Nyctaginaceae_Acleisanthes_obtusa_33521
Nyctaginaceae_Abronia_umbellata_59901
Nyctaginaceae_Commicarpus_scandens_9477
Nyctaginaceae_Cyphomeris_gypsophiloides_16268
Nyctaginaceae_Mirabilis_jalapa_AB435372.1_cds_BAG80686.1_1
Nyctaginaceae_Mirabilis_pringlei_33165
Nyctaginaceae_Mirabilis_multiflora_44341
Nyctaginaceae_Colignonia_ovalifolia_2171
Nyctaginaceae_Salpianthus_purpurascens_91019
Petiveriaceae_Monococcus_echinophorus_54274
Petiveriaceae_Rivina_humilis_15447
Phytolaccaceae_Anisomeria_littoralis_57030
Phytolaccaceae_Phytolacca_americana_24205
Agdestidaceae_Agdestis_clematidea_15017
Gisekiaceae_Gisekia_pharnaceoides_439
Aizoaceae_Conophytum_uviforme_DN6421_c0_g3_i2
Aizoaceae_Fenestrania_aurantiaca_DN19219_c0_g2_i2
Aizoaceae_Mesembryanthemum_crystallinum_Mecry_173920_CDS_-_McDODAa1
Limeaceae_Limeum_aethiopicum_DODAa
Chenopodiaceae_Anabasis_articulata_53850
Chenopodiaceae_Haloxylon_ammodendron_38175
Chenopodiaceae_Kali_collina_24381
Chenopodiaceae_Caroxylon_vermiculatum_87166
Chenopodiaceae_Eokochia_saxicola_53502
Chenopodiaceae_Suaeda_fruticosa_9702
Chenopodiaceae_Suaeda_linearis_1939
Chenopodiaceae_Kalidium_cuspidatum_23308
Amaranthaceae_Polycnemum_majus_4766
Chenopodiaceae_Spinacia_oleracea_Spo27232
Chenopodiaceae_Atriplex_hortensis_62354
Chenopodiaceae_Atriplex_sp_21625
Chenopodiaceae_Extriplex_californica_28742
Chenopodiaceae_Proatriplex_pleiantha_11096
Chenopodiaceae_Chenopodiastrum_murale_51976
Chenopodiaceae_Chenopodium_giganteum_Chenopodium_amaranticolor_14731
Chenopodiaceae_Oxybasis_rubra_6048
Chenopodiaceae_Krascheninnikovia_lanata_42646
Chenopodiaceae_Agriophyllum_squarrosum_33278
Amaranthaceae_Alternanthera_philoxeroides_86014
Amaranthaceae_Tidestromia_lanuginosa_35934
Amaranthaceae_Iresine_arbuscula_42789
Amaranthaceae_Iresine_rhizomatosa_38768
Amaranthaceae_Gossypianthus_lanuginosus_16893
Amaranthaceae_Guilleminea_densa_var_aggregata_15913
Amaranthaceae_Ptilotus_exaltatus_hyb_KF747354.1_cds_AIS23505.1_1
Amaranthaceae_Froelichia_latifolia_25043
Amaranthaceae_Tidestromia_lanuginosa_35931
Amaranthaceae_Alternanthera_philoxeroides_86019
Amaranthaceae_Nelsia_quadrangula_44223
Chenopodiaceae_Beta_vulgaris_XM_010675993.2_cds_XP_010674295.1_1
Chenopodiaceae_Beta_vulgaris_XM_010675996.2_cds_XP_010674298.1_1
Chenopodiaceae_Beta_vulgaris_HQ656022.1_cds_AET43288.1_1
Amaranthaceae_Amaranthus_hypochondriacus_HQ889614.1_cds_ADZ48644.1_1
Amaranthaceae_Amaranthus_tricolor_KP165399.1_cds_AJW81119.1_1
Amaranthaceae_Gossypianthus_lanuginosus_40105
Amaranthaceae_Tidestromia_lanuginosa_37237
Amaranthaceae_Nelsia_quadrangula_55789
Amaranthaceae_Amaranthus_cruentus_KM592963.1_cds_AJD87538.1_1
Amaranthaceae_Amaranthus_tricolor_18737
Chenopodiaceae_Caroxylon_vermiculatum_73089
Chenopodiaceae_Eokochia_saxicola_70762
Chenopodiaceae_Arthrocnemum_macrostachyum_57682
Chenopodiaceae_Beta_vulgaris_HQ656027.1_cds_AET43293.1_1
Chenopodiaceae_Chenopodium_quinoa_AUR62022991-RA
Chenopodiaceae_Spinacia_oleracea_XM_021991322.1_cds_XP_021847014.1_1
Chenopodiaceae_Chenopodium_quinoa_XM_021876909.1_cds_XP_021732601.1_1
Chenopodiaceae_Extriplex_californica_9479
Chenopodiaceae_Krascheninnikovia_lanata_31913
Amaranthaceae_Froelichia_latifolia_26247
Amaranthaceae_Tidestromia_lanuginosa_4485
Chenopodiaceae_Beta_vulgaris_XM_010676009.2_cds_XP_010674311.1_1
Chenopodiaceae_Oxybasis_rubra_10367
Chenopodiaceae_Oxybasis_rubra_36364
Caryophyllaceae_Cardionema_ramosissimum_DODAa
Caryophyllaceae_Polycarpon_tetraphyllum_DODAa
Caryophyllaceae_Spergularia_marina_DODAa
Achatocarpaceae_Achatocarpus_gracilis_8287
Caryophyllaceae_Telephium_imperatii_DODAa
Macarthuriaceae_Macarthuria_australis_DODAa
Stegnospermataceae_Stegnosperma_halimifolium_1183
Miroteaceae_Microtea_debilis_174616
Stegnospermataceae_Stegnosperma_halimifolium_50374
Chenopodiaceae_Chenopodium_quinoa_AUR62006956-RA
0.2